	HERCULES-2 Project *Fuel Flexible, Near Zero Emissions, Adaptive Performance Marine Engine*
	Deliverable: D2.4 MODELING OF MULTI-FUEL IGNITION Revision Final

Nature of the Deliverable:	Report
Due date of the Deliverable:	2018-04-30
Actual Submission Date:	2018-04-30
Dissemination Level:	Public

Contributors:	MDT
	DTU
	LUND
	POLIMI
Work Package Leader Responsible:	Johan Hult (MAN Diesel & Turbo)

	Start date of Project: 01/05/2015 Duration: 42months Grant Agreement No: **634135-HERCULES-2** **HORIZON 2020** The EU Framework Programme for Research and Innovation	

TABLE OF CONTENTS

1 Deliverable PART A

1.1 Executive summary

Alternative fuels are making their entrance into the maritime industry, as they are a viable alternative for complying with current and future engine emission regulations. Examples of fuels already being used or planned for include liquefied and compressed natural gas (LNG, CNG), ethane, methanol and liquefied petroleum gas (LPG). Numerical tools and models for describing and predicting alternative and multi-fuel combustion are crucial for designing and optimising marine engines capable of exploiting the full potential of these fuels. Here we will present the development of a chemical kinetic model describing these fuels, and the experimental work performed to validate the model. We will also demonstrate its use in engineering tools for ignition, flame speed and combustion simulations.

A high-pressure flow-reactor is used at DTU to investigate the oxidation properties of methane, ethane, ethanol, propane, and butane at high pressures (20–100 bar) and intermediate temperatures (450–900 K). The experiments reveal the onset of fuel oxidation at temperatures starting from 600 K up to 825 K, depending on pressure and fuel-air equivalence ratios. It was found that the oxidation of both methane and ethane starts around 750 K (100 bar, stoichiometric mixture) while propane and butane are oxidized at lower temperatures of 600–700 K (100 bar, stoichiometric mixture). Ethanol is oxidized at 700 K if the pressure is 50 bar.

The data collected from the flow-reactor is used to develop a detailed chemical kinetic model for the combustion of aforementioned fuels at pressures and temperatures relevant to marine engine operating conditions. For instance, Figure 19 shows the gas composition at the flow-reactor outlet for a methane oxygen mixture under stoichiometric conditions for different isotherms. The model reproduces accurately the onset of reaction as well as the relative changes in the fractions of stable components. However, it underpredicts the conversion of methane and oxygen at high temperatures, accompanied by an underprediction of CO_2.
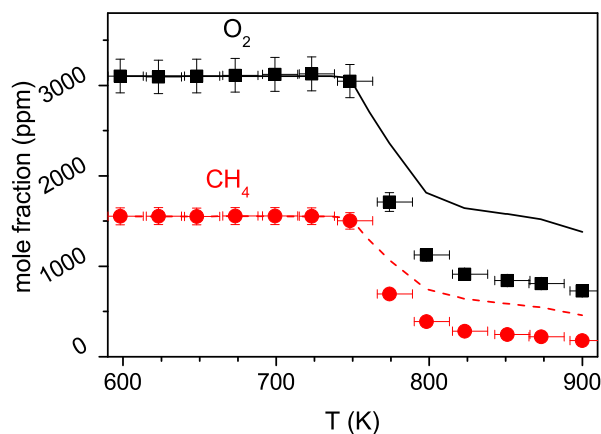

Figure 1: Results for methane under stoichiometric conditions (Φ=1.0) at 100 bar. Symbols mark the experimental results and lines denote the predictions of the developed detailed chemical kinetic model.

The developed model is further evaluated against existing data in literature. Flame speed and ignition delay time predictions are especially evaluated due to their importance for:

- capturing key physics using Computational Fluid Dynamics (CFD) low-dimensional engineering tools.

- performing accurate multi-dimensional CFD calculations.

In general, the model could predict the oxidation properties of aforementioned fuels reasonably well as shown in Figure 20 for methane ignition delay time.
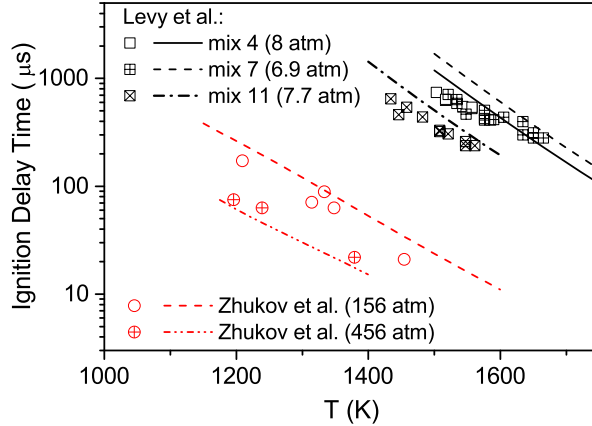

Figure 2: Ignition delay times of CH_4/air (Φ=0.5, from Zhukov et al. [1]) and CH_4/O_2 mixtures (from Levy et al. [2], mix 4: 3.53% CH_4 in N_2, 8 atm, Φ=1.01; mix 7: 4.0% CH_4 in N_2, 6.9 atm, Φ=1.33; mix 11: 1.99% CH_4 + 3.72% CO_2 in N_2, 7.7 atm, Φ=0.32). The simulations are conducted at fixed pressures while the pressure in the experiments fluctuated within $\pm 10\%$.

This comprehensive evaluation of the model and its application range is described in this report. The improvement of the model prediction for propane and butane as well as the evaluation of the model against measured flame data for propane are currently under further investigations.

This detailed chemical kinetic model is then used as the basis of two engineering tools, developed at MDT, that allow a quick evaluation of respectively the ignition delay time and the laminar flame speed of various fuel composition under engine-like conditions. These tools can also be used to create ignition table for example. They are based on the open-source software Cantera [3] and Python programming language.

Finally a proof of concept for direct integration of chemical kinetic models into a multi-dimensional CFD simulation for dual fuel was conducted for a methanol–diesel configuration as show in Figure 3. Although OpenFOAM is found to be a very good tool for such study, it was concluded that direct integration of the developed detailed chemical kinetic model into a multi-dimensional CFD simulation of dual fuel is still found to be prohibitive and beyond the reach of industrial application without further reduction. A few conventional methods to reduce detailed chemical kinetic models to skeletal ones are currently being tested in order to identify the most suitable approach. As part of this work package extension, other approaches, based on the developed detailed (or skeletal) chemical kinetic model, are explored in order to simulate accurately multi-fuel combustion

using multi-dimensional CFD. A strong focus is also given on the charge preparation prior to combustion and on the overall computational efficiency in manipulating complex engine meshes. These results will be documented in deliverable D2.4 PART B, with proposed submission M42.
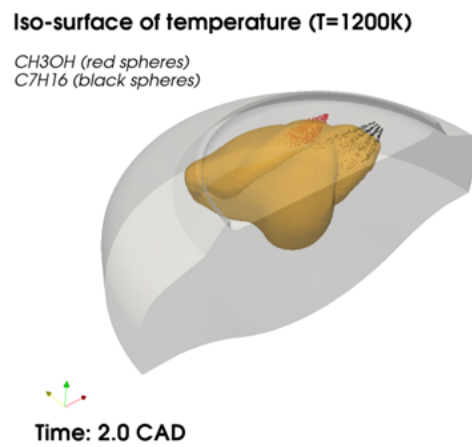

Figure 3: Iso-surface of temperature (T=1200 K) at 2.0 CAD for a dual-fuel CH_3OH (red) and C_7H_16 (black) combustion using a two steps reaction chemical kinetic model. Proof of concept simulation is performed in OpenFOAM.

1.2 Introduction

Climate change has become a serious concern nowadays. The main reason of the current changes in the climate is believed to be the high emission of greenhouse gases mainly from human activities. The energy demand has increased exponentially [4] and even though the fuel efficiency improved globally, the CO_2 emission has increased considerably [4]. The steady increase in the global energy demand as well as in the release of carbon dioxide and other harmful pollutants from the combustion of most fossil fuels are the major motivations to seek alternative sources of energy. In a mid-term prospect, fuels which produce less pollutants and CO_2, and have a higher energy efficiency may relieve the environmental problems to some extent. For marine applications, alternative fuels such as Liquefied and Compressed Natural Gas (LNG and CNG), ethanol and Liquefied Petroleum Gas (LPG) are currently among the most viable options. In a global transportation system, these fuels might be supplied in various compositions and/or purity which effects should be accounted for. Methane (CH_4) and ethane (C_2H_6) are the major components in LNG and CNG. Neat ethane can also be used as an engine fuel for ships transporting feedstock ethane. Propane (C_3H_8) and butane (C_4H_{10}) are the major component of LPG. Trace amounts of propane and butane can be also found in natural gas. The variations in CH_4, C_2H_6, C_3H_8, and C_4H_{10} fractions can affect the ignition, oxidation, and pollutant formation of the given fuels considerably. Experimental study of the effects of changing fuel in practical conditions are not always economic or even feasible, which emphasizes the role of modelling in design/optimization of engines. Computational Fluid Mechanics (CFD) modelling approaches can range from engineering low dimensional tools, typically 0-Dimension (0-D) or 1-Dimension (1-D), as investigated in this project to multi-dimensional simulations (3-Dimensions). Theoretically, the most accurate approach to model ignition and combustion in engines is to use 3-D CFD calculations coupled with detailed or simplified chemical kinetic schemes but the computational requirements are out of rich in an industrial framework. Ignition, as a potentially challenging issue in the combustion of alternative fuels, is mainly governed by chemical kinetics. Thus a reliable chemical kinetic model is a critical block for the CFD modelling used for the design and optimization of combustion devices. Such a model usually consists of a large number of reactions and species and in order to evaluate either detailed or simplified version of such a model, it is necessary to compare the prediction of chosen combustion parameters with experimental measurements. For example, the oxidation properties of propane and butane have attracted research and industrial interests as, for both of them, oxidation exhibits a non-linear trend to temperature over a certain range of temperature. To better reveal the chemical details, it is desirable to avoid turbulent combustion and to simplify the flow field as much as possible [5]. The evaluating parameters, *combustion characteristics*, should be independent from device and configurations. Species evolution profiles, ignition delay times, and laminar burning velocities are more frequently used as combustion characteristics. Species evolution profiles can be measured in flow reactors, jet-stirred reactor, shock tubes, and rapid compression machines (RCM). To measure ignition delay times, shock tubes and RCM have been used more frequently. Different configurations of burners and constant-volume test vessels are used to quantify the flame speed of gas mixtures.

As mentioned previously, detailed models usually consist of a large number of reactions

and species. Despite the rapid growth in computational capabilities, direct implementation of large chemical schemes in multi-dimensional CFD calculations is prohibitive. The computational cost will escalate for practical multi-components fuels where their reaction kinetic models include hundreds of species and thousands of reactions. To address this problem, several approaches can be considered. A direct integration of a simplified description of chemistry can be used. Such simple models were expected to fairly reproduce selected aspects of combustion, e.g. ignition or pollutant emission under a given operating range. The calculation speed up can be further increased by using an additional strategy such as Chemistry Coordinate Mapping (CCM). Another approach is to use tabulated chemistry model in CFD where the tables are generated from a detailed chemistry model. Within WP2, MDT proposed to significantly boost the multi-fuel modelling capabilities, by supporting activities with research groups located at two existing partners: Politecnico di Milano (WP5 partner) and Lund University (already WP2 partner). These results will be documented in deliverable D2.4 PART B, with proposed submission M42.

1.3   Objectives

The objective is to develop the numerical tools required to exploit new alternative fuels in future marine engines. In order to operate efficiently on a larger variety of fuels an increased understanding of ignition, combustion and emissions formation of those novel or mixed fuels is required. Numerical tools can provide insight in ignition and emission formation. Detailed chemical kinetic models evaluated against experimental data at conditions relevant for marine engines are required to develop such tools. Experimental measurements will be conducted in a high-pressure flow-reactor facility in DTU Chemical Engineering to facilitate model development and evaluation.

Within the work package extension framework, it is also expected that

- POLIMI is to apply and evaluate methods, mesh handling and models initially developed for the automotive industry in a large two-stroke marine engine framework. Especially the mesh handling and turbulence prediction will be complementary to the support of LUND on detailed chemistry.

- LUND will first evaluate the CCM approach in case of multi-fuels combustion in a large two-stroke Diesel engine. Then the effect of turbulence chemistry interaction will be investigated by means of a pdf approach.

- Investigations by all partners on simulation speed-up techniques are expected as well.

1.4 Detailed chemical kinetic models

1.4.1 The laminar flow reactor

The experimental setup was a laboratory–scale, high–pressure laminar flow reactor designed to approximate plug flow. It has been described in detail elsewhere [6] and only a brief description is provided here. The system was used to investigate fuels oxidation chemistry at 20–100 bar pressure and temperatures up to 900 K. The reactions took place in a tubular quartz reactor (inner diameter of 8 mm), enclosed in a stainless steel tube that acted as a pressure shell. Using a quartz tube and conducting the experiments at high pressure ensured a minimal contribution from heterogeneous reactions at the reactor wall. The steel tube was placed in a tube oven with three individually controlled electrical heating elements that produced an isothermal reaction zone (± 6 K) of 37–43 cm. A moving thermocouple was used to measure the temperature profile inside the pressure shell wall after stabilizing the system. The system was pressurized from the feed gas cylinders. The reactor pressure was monitored upstream of the reactor by a differential pressure transducer and controlled by a pneumatically actuated pressure-control valve positioned after the reactor. The pressure fluctuations were less than 0.2 % during the experiments. The reactant gases were premixed before entering the reactor. Downstream of the reactor, the system pressure was reduced to atmospheric level prior to product analysis, which was conducted by an on-line 6890N Agilent Gas Chromatograph (GC-TCD/FID from Agilent Technologies). All Gas Chromatograph (GC) sampling and measurements were repeated at least twice to reduce uncertainties in measurements. For gaseous compounds the GC peak areas were related to concentrations by calibration against certified gas mixtures ($\pm$ 2% from AGA A/S). A general uncertainty of 6% is estimated for measurements by GC. Figure 4 shows the measured temperature profiles for different isotherms with a flow of pure nitrogen. The uncertainty in the gas temperature due to the effect of heat release
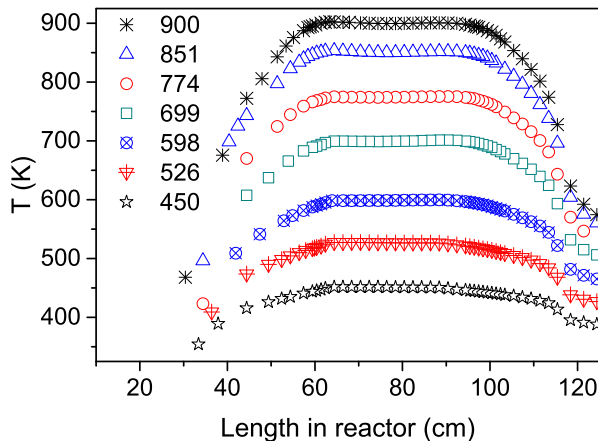
Figure 4: Temperature profiles along the reactor length for different isotherms with nitrogen flow.

from combustion was limited by a high level of dilution. Because of the fast heat transfer from the hot gases to the pressure shell, augmented by the small dimensions of the reactor, we estimate the deviation of the gas temperature from the measured temperature to be negligible. Measurement of the wall temperature in real experiments did not reveal

any deviation beyond ±2 K.

1.4.2 Methane

Oxidation mechanisms for methane are available [7–11], but they have mostly been verified at lower pressure and/or higher temperature. In shock tubes, ignition delays for CH_4 have been obtained over a wide pressure range [1, 2, 12–14], but shock tube studies are generally restricted to temperatures above 1100 K. Even at high temperatures, autoignition depends not only on chemical processes at the time of ignition, but also on the earlier, lower temperature chemistry creating the necessary conditions for ignition [15]. The relatively long residence times, which are required to study combustion at high pressures and temperatures of 600-1100 K can be realized in static reactors and flow reactors.

In the present work we conduct methane oxidation experiments in a laminar flow reactor at 700–900 K and 100 bar. A detailed chemical kinetic model is established, drawing on the previous high-pressure work [6, 7, 16–19], and modeling predictions are compared with the present measurements as well as data from shock tubes and flames at the highest pressures reported. Details of the methane oxidation model can be found in [20].

Oxidation in the flow reactor

The developed model for methane has been evaluated against experimental data measured in the DTU's high-pressure flow-reactor. Figure 5 shows the gas composition at the reactor outlet under stoichiometric conditions for different isotherms. Under these conditions, the fuel conversion starts at a temperature of 750 K. The model reproduces accurately the onset of reaction as well as the relative changes in the fractions of stable components. However, it underpredicts the conversion of methane and oxygen at high temperatures, accompanied by an underprediction of CO_2.

The experiments were repeated for fuel-rich (reducing conditions, $\Phi=19.7$) and fuel-lean (oxidizing conditions, $\Phi=0.06$) mixtures. The model generally agrees well with the measurements. Further details of the comparison can be found in A.
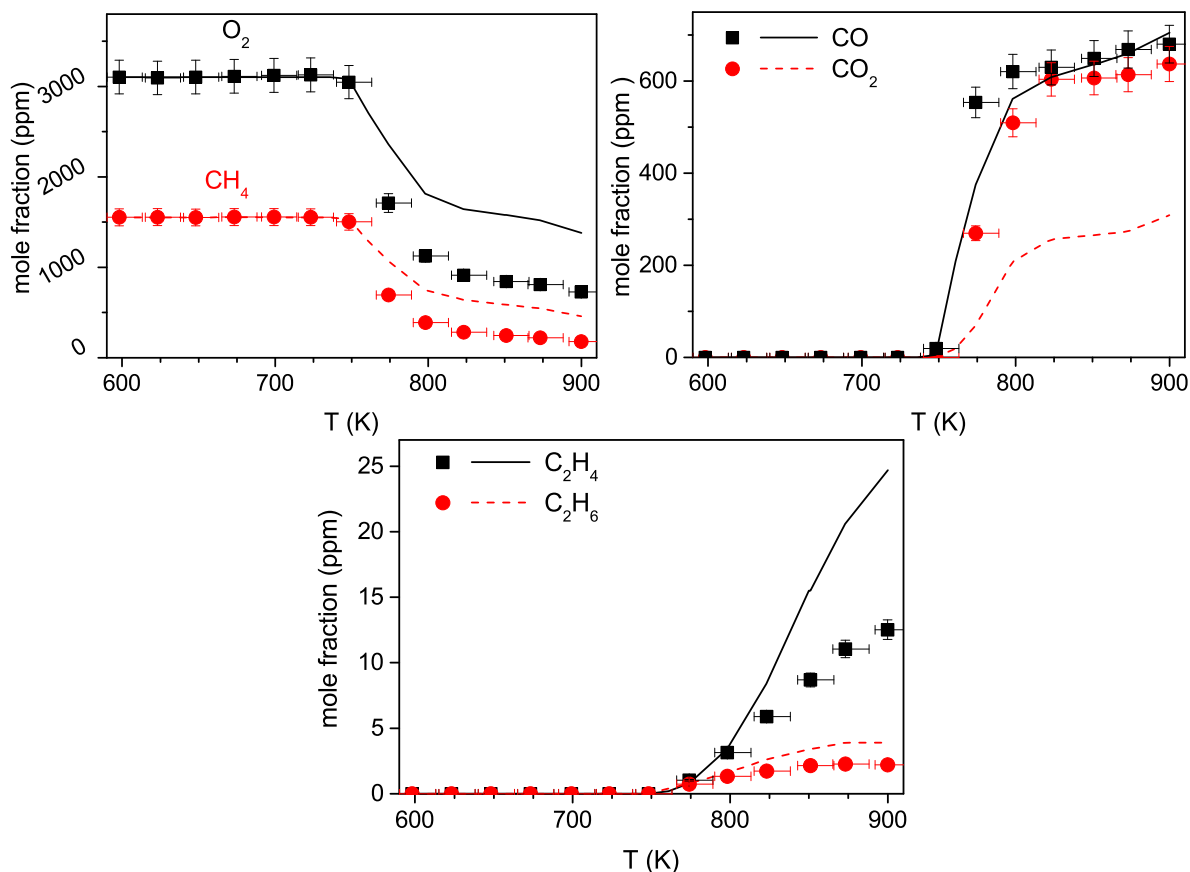
Figure 5: Results of experiments under stoichiometric conditions (0.31% O_2 and 0.16% CH_4 in N_2, Φ=1.0) at 100 bar pressure. Symbols mark the experimental results and lines denote the predictions of the present model. The temperature profile was implemented in the simulations. Considering only the isothermal zone of the reactor ($\pm$ 6 K, residence time=9586/T [s]) deteriorates slightly the agreement.

Ignition delay time in shock tubes

The oxidation of methane has been investigated extensively in shock tubes [1, 2, 12, 14, 21–32]. In Fig. 6, modeling predictions are compared to selected ignition delay data obtained at very high pressure by Zhukov et al. [1]. As shown the modeling results agree well with the measured data at 156 and 456 atm. The figure also includes ignition delays measured at much lower pressures (6.9–8.0 atm) by Levy et al. [2]. Detailed comparison of the results of the present model with the literature data can be found in A.

11

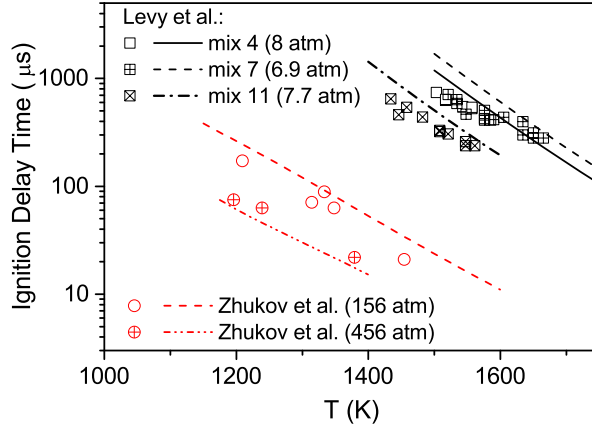Figure 6: Ignition delay times of CH_4/air (Φ=0.5, from Zhukov et al. [1]) and CH_4/O_2 mixtures (from Levy et al. [2], mix 4: 3.53% CH_4 in N_2, 8 atm, Φ=1.01; mix 7: 4.0% CH_4 in N_2, 6.9 atm, Φ=1.33; mix 11: 1.99% CH_4 + 3.72% CO_2 in N_2, 7.7 atm, Φ=0.32). The simulations are conducted at fixed pressures while the pressure in the experiments fluctuated within ±10%.

Flame speed

The laminar burning velocity of methane has been measured in several studies [33–39], but most of the published data are limited to low pressure. Figure 7 compares simulations with the experimental data. As expected, the flame speed decreases at elevated pressures. The predicted flame speeds agree well with the measurements at pressures of 1, 5, and 10 atm.
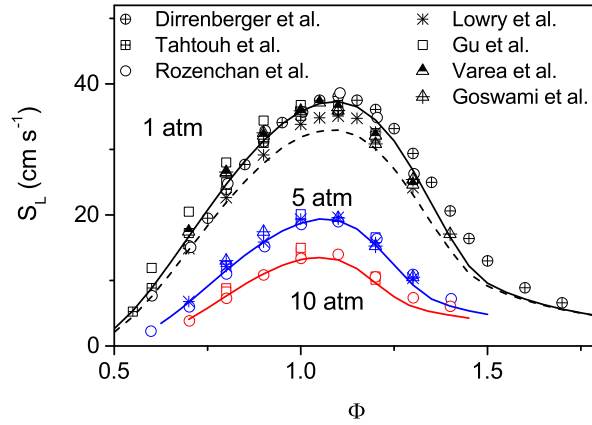
Figure 7: Laminar burning velocity of methane/air mixture at 1, 5, and 10 atm and initial temperature of 298–300 K. Symbols mark experimental results from Gu et al. [33], Dirrenberger et al. [34], Rozenchan et al. [35], Varea et al. [36], Goswami et al. [37], Tahtouh et al. [38], and Lowry et al. [39]. Lines denote the model prediction at specified pressures. The dashed line corresponds to modeling without inclusion of the prompt dissociation of HCO.

1.4.3   Ethane

From a fundamental perspective, the oxidation of C_2H_6 plays an important role in the hierarchical structure of the reaction mechanisms of hydrocarbon fuels. To develop and verify these chemical kinetic models for hydrocarbon oxidation, measurements of the combustion characteristics at high pressure are essential.

While hydrocarbon ignition even at high temperatures relies on intermediate temperature chemistry, this range of temperature, particularly at high pressure, has only been sparsely studied. However, pressures investigated in these studies are still below those relevant for modern internal combustion engines.

To extend the available data toward conditions relevant to engines, this work reports the results of ethane oxidation experiments in a laminar flow reactor at pressures of 20–100 bar and temperatures of 600–900 K under a wide range of stoichiometries. A chemical kinetic model for ethane oxidation at increased pressure was established. Details of the developed model can be found in [40].

Oxidation in the flow reactor

The flow-reactor tests were carried out at pressures of 20, 50, and 100 bar to survey the effects of pressure-dependent reactions. The mixture composition has been changed from extreme fuel-rich conditions to stoichiometric and then fuel-lean conditions to represent the wide range of stoichiometries observed in engines. Here, the results from stoichiometric tests are presented while data for fuel-lean and fuel-rich mixtures can be found in B.

For near-stoichiometric mixtures (ϕ=0.81–0.91), the onset of fuel oxidation is at temperatures of 825, 775, and 750 K for pressures of 20, 50, and 100 bar, respectively (Fig. 8). The major products are CO, CO_2 and C_2H_4, with C_2H_4 disappearing at increased temperature. The model predictions agree very well with the measurements. From the experiments, it can be seen that when pressure is increased, the fuel oxidation starts at lower temperatures.

Ignition delay time in shock tubes

The ignition delay time of ethane has been measured at pressures greater than 10 atm in several shock tube studies [25, 41–43]. Figure 9 shows the measured ignition delay times and the predictions by the present model. The modelling predictions compare reasonably well with the measured values.

Flame speeds

For ethane/air mixtures, the flame speed has been measured at pressures up to 10 atm [39, 44–49]. Figure 10 compares modelling predictions with measurements at 1, 5, and 10 atm. The model overpredicts the flame speed by up to about 5 cm s^{-1} for fuel-lean and stoichiometric mixtures, but its accuracy improves for fuel-rich mixtures.
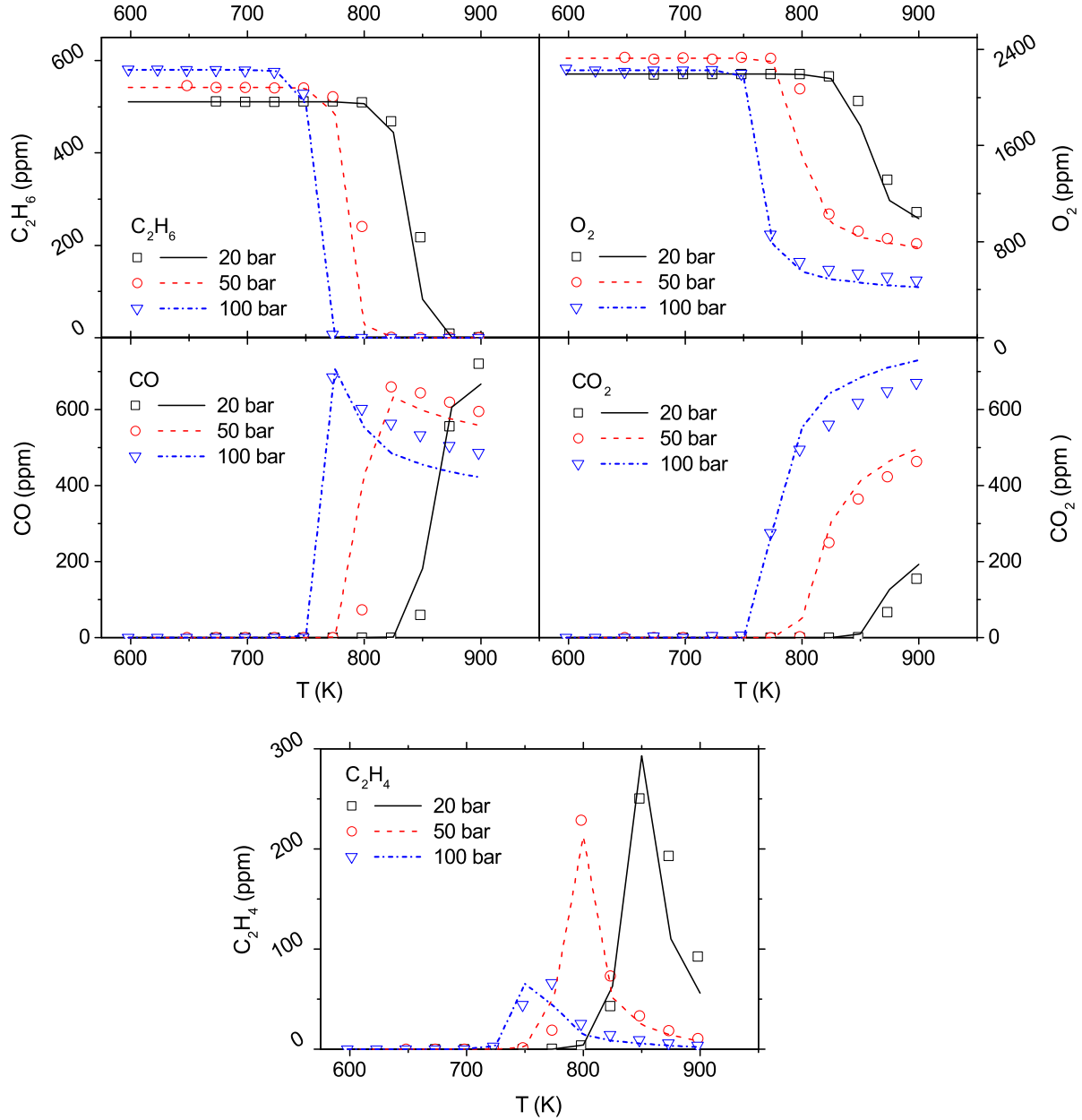
Figure 8: Results (molar fractions) of experiments under stoichiometric conditions at 20 bar (ϕ=0.82, 511/2194 ppm of C_2H_6/O_2), 50 bar (ϕ=0.81, 542/2328 ppm of C_2H_6/O_2), and 100 bar (ϕ=0.91, 580/2228 ppm of C_2H_6/O_2). All mixtures are diluted in nitrogen. Symbols mark experimental results and lines denote predictions of the present model using the temperature profiles in the supplementary materials. Approximating the gas residence time by τ=2580/T [K] s (20 bar), τ=6170/T [K] s (50 bar), and τ=12830/T [K] s (100 bar) may deteriorate the model predictions slightly.
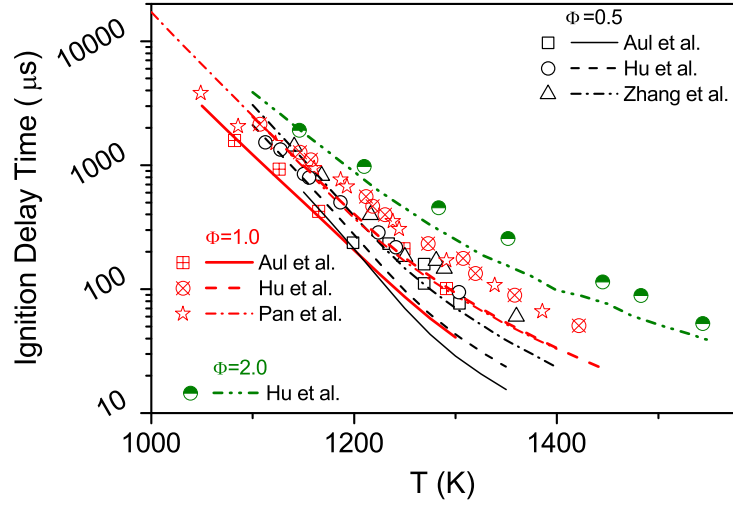
Figure 9: Ignition delay time of $C_2H_6/O_2/Ar$ mixtures calculated by the present model. Symbols mark experimental results from Aul et al. [25] (85% Ar, 16 atm), Zhang et al. [41] (95% Ar, 21 atm), Pan et al. [42] (95% Ar, 16 atm), and Hu et al. [43] (1% C_2H_6 in Ar, 20 atm).
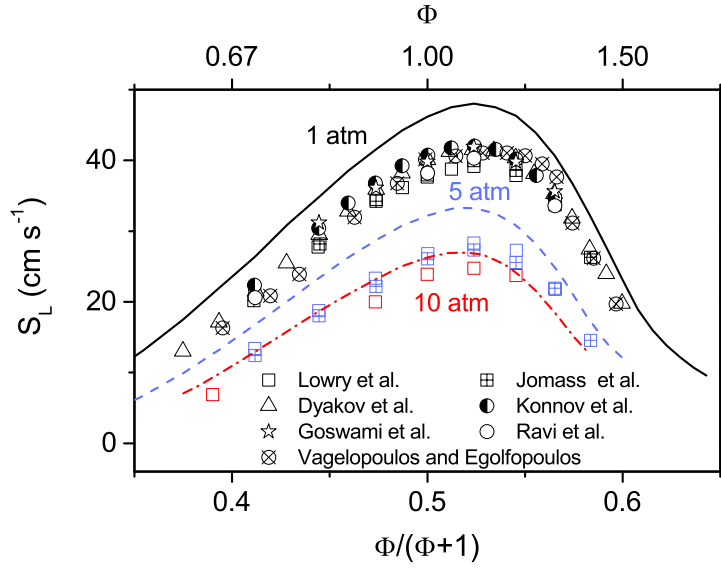
Figure 10: The unstretched laminar burning velocity of ethane/air mixtures versus normalized equivalence ratio for an initial temperature of 300 K and at different pressures. Lines denote the present model predictions and symbols mark experimental results from Lowry et al. [39], Vagelopoulos and Egolfopoulos [44], Konnov et al. [45], Jomaas et al. [46], Dyakov et al. [47], Goswami [48], and Ravi et al. [49].

1.4.4 Propane

Propane oxidation exhibits a non-linear trend to temperature over a certain range of temperature; the oxidation is inhibited by increasing temperature. This behaviour, more frequent in heavier fuels, is called NEGATIVE TEMPERATURE COEFFICIENT (NTC). The NTC trend increases the complexity of reaction mechanism and ignition modelling. The temperature range at which NTC is observed in propane oxidation depends on pressure and mixture composition, but generally NTC is found at T<1200 K. Flow reactors are one of the suitable devices to investigate combustion chemistry at intermediate temperatures. However, propane oxidation experiments in flow reactors have been limited to [50, 51] with P<15 atm. The ignition delay time of propane has been investigated to a larger extent due to its complex behavior. Data collected at relatively high pressures are those reported in [26, 52–57] for P<40 atm, which is still away from pressures in engines.

In the present work we conduct propane oxidation experiments in a laminar flow reactor at 450–900 K and 100 bar. A detailed chemical kinetic model is established, based on previous high-pressure work [6, 7, 16–20, 40], and modelling predictions are compared with the present measurements as well as data from shock tubes and flames at the highest pressures reported. Details of the model for propane oxidation can be found in [58].

Oxidation in the flow reactor

Figure 11 shows the results of propane oxidation for a stoichiometric mixture. The fuel conversion started around 725 K, where a small fraction of propane disappeared while trace amounts of C_3H_6 and C_2H_4 were detected. Propane was oxidized almost completely at T>750 K. The model captured the onset temperature of ignition accurately. However, it seems that CO oxidation to CO_2 at high temperatures was not precisely captured by the model.

The experiments were repeated for fuel-rich (reducing conditions, Φ=12.5) and fuel-lean (oxidizing conditions, Φ=0.02) mixtures. The model generally agrees well with the measurements. Further details of the comparison can be found in C.
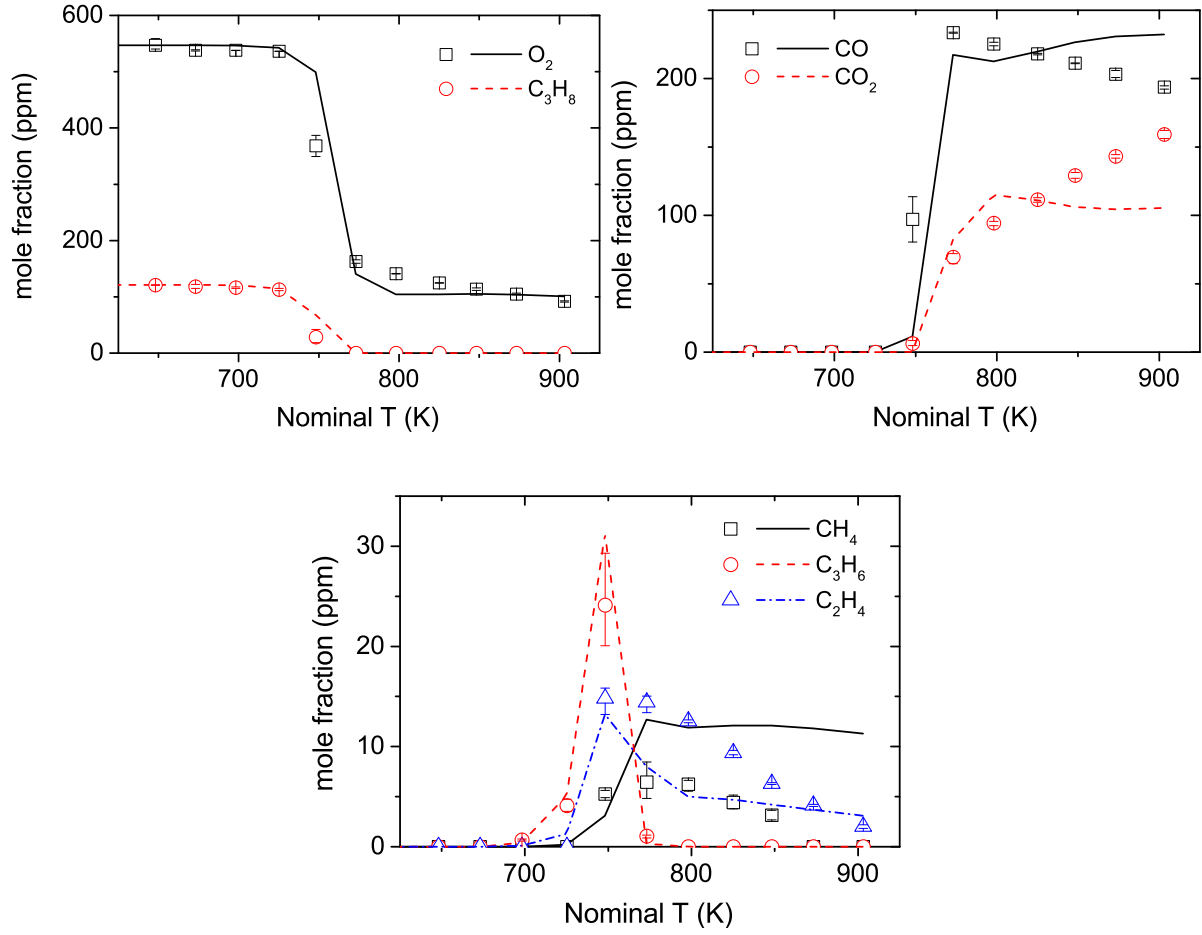
Figure 11: Results of experiments under stoichiometric conditions (547 ppm O_2 and 121 ppm C_3H_8 in N_2, Φ=1.1) at 100 bar pressure. Symbols mark the experimental results and lines denote the predictions of the present model. The temperature profile was implemented in the simulations.

Ignition delay time in shock tubes

Ignition delays of propane have been measured in shock tubes at P<40 atm [52, 53]. The prediction of the present model is compared with literature data in Fig. 12. Although the model overestimates ignition delays at T<1100 K, its prediction improves at higher temperatures. The deviation of the model might be due to large uncertainty of ignition delays measured at τ >1 ms in shock tubes due to pre-ignition pressure rise. This problem has been discussed in [20, 59]
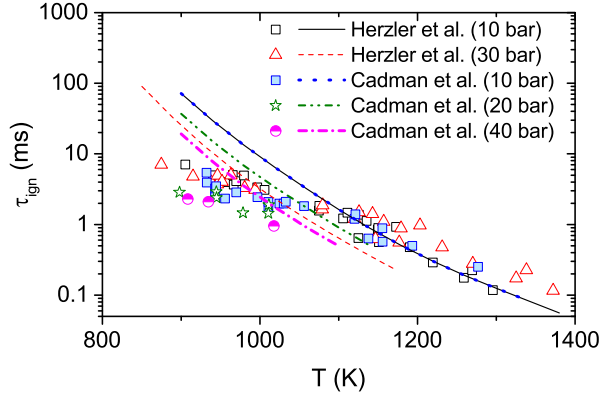
Figure 12: Ignition delay times of propane/oxygen/nitrogen mixtures (2.1% C_3H_8 + 20.6% O_2 in N_2, Φ=0.5) at 10–40 bar. Symbols mark experimental results from Herzler et al. [53] and Cadman et al. [52] and lines denotes the predictions of the present model.

1.4.5 Butane

Butane ignition was investigated at pressures up to 45 bar [60–62], which is still below the pressure in modern engines.

In the present work we conduct butane oxidation experiments in a laminar flow reactor at 450–900 K and 100 bar. A detailed chemical kinetic model is established, based on previous high-pressure work [6, 7, 16–19], and modelling predictions are compared with the present measurements as well as data from shock tubes and flames at the highest pressures reported. Details of the model for butane oxidation can be found in [59].

Oxidation in the flow reactor

The developed model for butane (normal butane) has been evaluated against experimental data measured in the DTU's high-pressure flow-reactor. The mixture composition has been changed from extreme fuel-rich condition to stoichiometric and then fuel-lean conditions to represent the wide range of stoichiometries observed in engines. Figure 13 shows the result for a stoichiometric mixture. A slight NTC trend can be observed between two inflection points in butane profile at 625 and 675 K. This trend is also reflected in oxygen profile. Even though the model underestimates slightly the concentrations of oxygen and butane between the inflection points, it predicts the onset of oxidation at 100 bar precisely. A major problem in the model prediction is due to the considerable underprediction of CO_2 fraction.
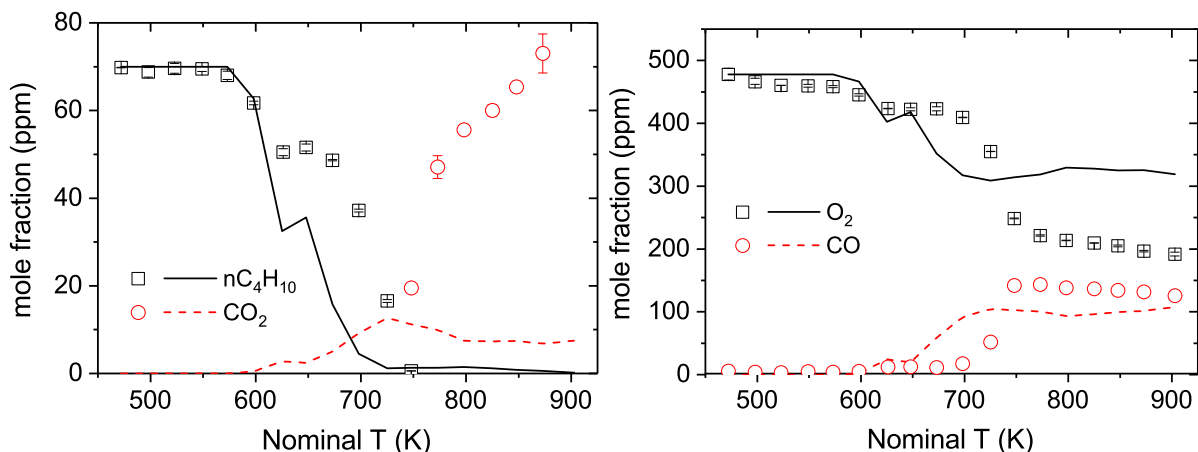
Figure 13: Results of experiments under stoichiometric conditions at 100 bar pressure (478 ppm O_2 and 70 ppm nC_4H_{10} in N_2, Φ=0.95). Symbols mark the experimental results and lines denote the predictions of the present model. The temperature profile was implemented in the simulations.

1.4.6 Ethanol

The reaction mechanism of ethanol is a crucial part in models for heavier alcohols often found in complicated biofuels [5]. Despite its importance, detailed data for ethanol oxidation at high pressures and intermediate temperatures are scare.

In this work we report species concentration profiles from ethanol pyrolysis and oxidation in a flow reactor at high pressure and intermediate temperatures. A detailed chemical kinetic model based on earlier studies from our laboratory [6, 7, 17, 18, 20, 40, 63, 64] is further developed and evaluated against the data from the present work as well as from literature. Details of the ethanol oxidation model can be found in [65].

Oxidation in the flow reactor

Under stoichiometric conditions, ethanol oxidation starts around 725 K. The major detected products are CO and CO_2, as shown in figure 14. The CO concentration peaks around 750 K and drops gradually at higher temperatures. Aldehydes are detected around 725 K, but they disappear at higher temperatures. Ethene, detected in a few ppm, shows a non-monotonic behaviour toward temperature.

The model reproduces fairly well the onset of fuel conversion as well as the concentration of major products. Notwithstanding CO is overestimated at high temperatures, the non-linear changes in aldehydes and ethene profiles are well predicted by the model.

The experiments were repeated for fuel-rich (reducing conditions, Φ=43) and fuel-lean (oxidizing conditions, Φ=0.1) mixtures. The model generally agrees well with the measurements. Details of the comparison to the flow-reactor data as well as ignition delays and flame speed from literature can be found in D.
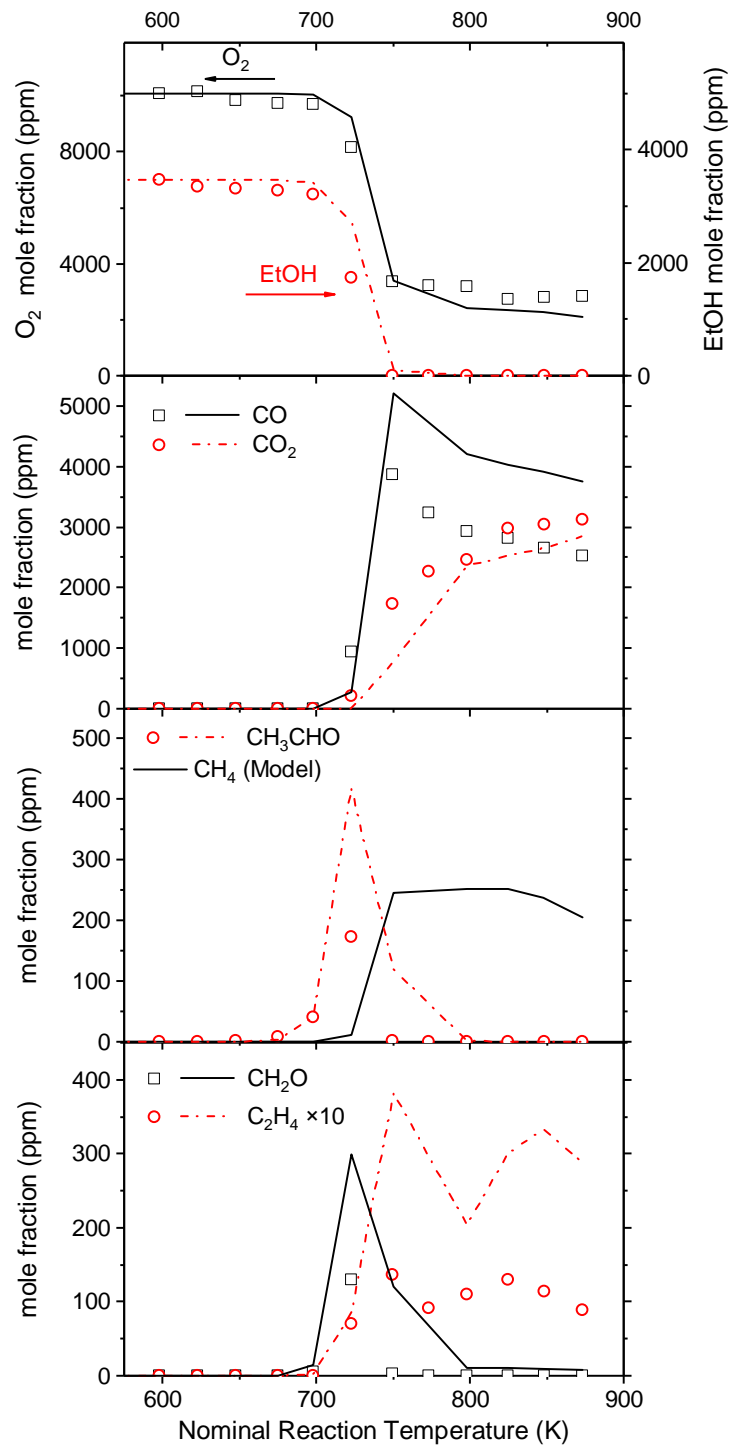
19

Figure 14: Results of experiments under stoichiometric conditions (0.3467% ethanol and 1.01% O_2 in N_2, Φ=1.0) at 50 bar. Gas residence time is given by τ[s]=3840/T[K] ($\pm$8%).

1.4.7 Summary

This comprehensive evaluation of the model and its application range is summarized in Table 1.

Table 1: Evaluation conditions of the developed mechanism.

Model	No. of Spec.	No. of React.	Fuel	Evaluated Parameter	Range of T [K]	Range of P [atm]
				Evaluation conditions		
DTU-C2	68	665	Methane	Components evolution [a]	600–900	100
				Ignition delay (RCM)	800–1250	15–80
				Ignition delay (Shock tube)	900–1800	7–456
				Flame speed		1–10
			Ethane	Components evolution [a]	600–900	20–100
				Components evolution [b]	1000–1500	40–613
				Ignition delay (RCM)	900–1025	10–80
				Ignition delay (Shock tube)	1000–1500	16–21
				Flame speed		1–10
			Ethanol	Components evolution [a]	600–900	50
				Ignition delay (RCM)	800–1000	10–50
				Ignition delay (Shock tube)	1000–1600	10–77
				Flame speed		1–12
DTU-C3	133	1114	Propane	Components evolution [a]	500–900	100
				Ignition delay (Shock tube)	900–1400	10–40
DTU-C4	236	1626	Butane	Components evolution [a]	500–900	100

[a] measured in DTU high-pressure flow-reactor
[b] measured in shock tubes

1.5 Using detailed chemical kinetic models

1.5.1 Engineering tool for ignition delay time evaluation

An engineering tool based on Cantera [3] and Python programming language has been created for ignition delay time calculations of various fuel mixture under various conditions. This tool makes direct use of the detailed chemical mechanisms developed by DTU in this work package. Figure 15 presents an example of such calculation for methane where the ignition delay time is evaluated for a given range of temperature and equivalence ratio at 100 bar. This tool can be used to create ignition table of various fuel (depending of the mechanism used) for CFD application.
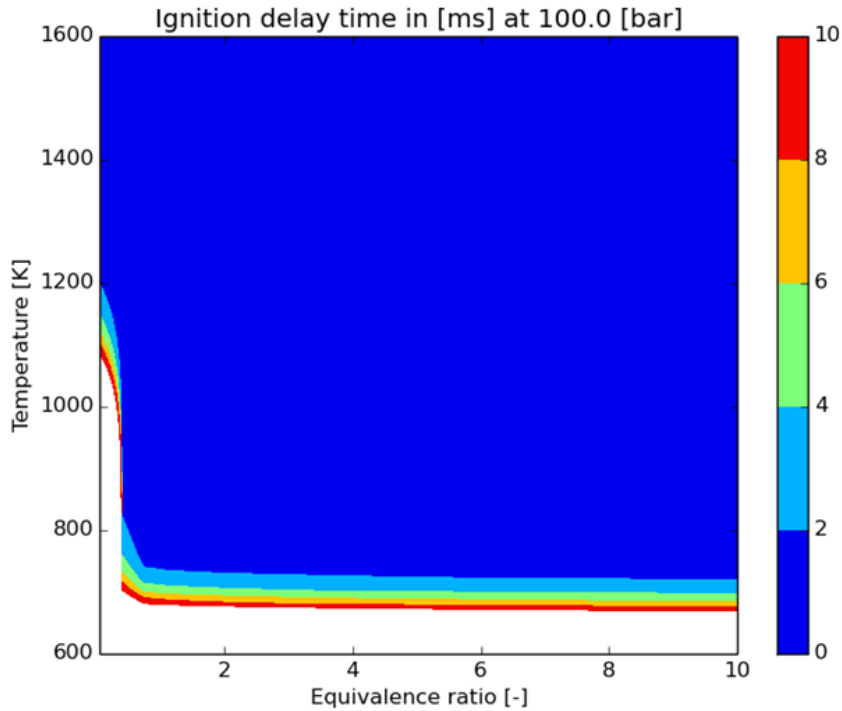
Figure 15: Example of calculation of ignition delay time for methane (CH$_4$) at 100 bar as a function of equivalence ratio (Φ) and temperature (without EGR)

1.5.2 Engineering tool for laminar flame speed evaluation

Similarly, a tool was developed in order to evaluate the laminar flame speed (Sl) under various conditions and mixtures. As shown in Table 2, it was first used to evaluate the difference in Sl calculation between between DTU and GRI3.0 mechanisms for methane at 1 bar and 300K (far from engine like conditions). It is worth noticing that the simulation time is significantly increased with the mechanism size as it takes about 10 min for GRI3.0 per Φ while it takes about 60 min for DTU per Φ. Despite the differences observed at low pressure and temperature, it is found that the DTU-C2 model performance at high pressure and temperature is good and validated. This tool currently requires manual

input to improve the stability of the calculations at high temperature or high pressure conditions.

Table 2: Example of laminar flame speed calculation for methane (CH_4) at 1 bar as a function of equivalence ratio (Φ) and temperature (without EGR)

| Model | Pressure [bar] | Temperature [K] | Mixture composition | | | | Sl [m/s] |
			CH_4 [mole]	O_2 [mole]	AR [mole]	N_2 [mole]	
DTU-C2	1.	300.	0.8	2	0	7.52	0.213
GRI3.0	1.	300.	0.8	2	0	7.52	0.272
DTU-C2	1.	300.	1.	2	0	7.52	0.316
GRI3.0	1.	300.	1.	2	0	7.52	0.378
DTU-C2	1.	300.	1.3	2	0	7.52	0.223
GRI3.0	1.	300.	1.3	2	0	7.52	0.234

1.5.3 Direct CFD integration: proof of concept

A detailed chemistry solver with multi-fuel injections was build in OpenFOAM allowing to read any chemical kinetic model as well as different liquid fuel specifications. The solver was tested in a simple setup involving combustion of methanol (CH_3OH) and n–heptane (C_7H_{16}) as Diesel surrogate. The reaction was modelled with a two steps reaction mechanism as described below:

$$C_7H_{16} + 11O_2 \rightarrow 7CO_2 + 8H_2O \tag{1}$$

$$2CH_3OH + 3O_2 \rightarrow 2CO_2 + 4H_2O \tag{2}$$
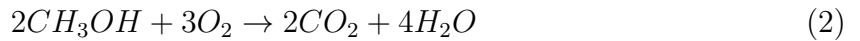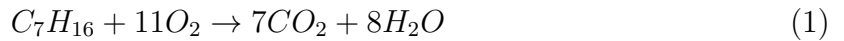
The chemical reaction rates (mainly for Reaction 1) were tuned to roughly reproduce the ignition delay time of a given mixture under the engine conditions at start of injection. However it should be noted that this simplified approach does not intend to reproduce the combustion process as it is far too simplified and inaccurate. It is a proof of concept.

The simulation was performed from -10 CAD up to 60 CAD. Figure 16 shows the methanol and n–heptane mass fraction at TDC as well as temperature iso-surface at 2 CAD and 4 CAD. Within this proof of concept framework, the results of the simulation seemed qualitatively acceptable. Moreover OpenFOAM is found to be an appropriate tool for such work and a simulation process was defined for future multi-fuel combustion simulation.
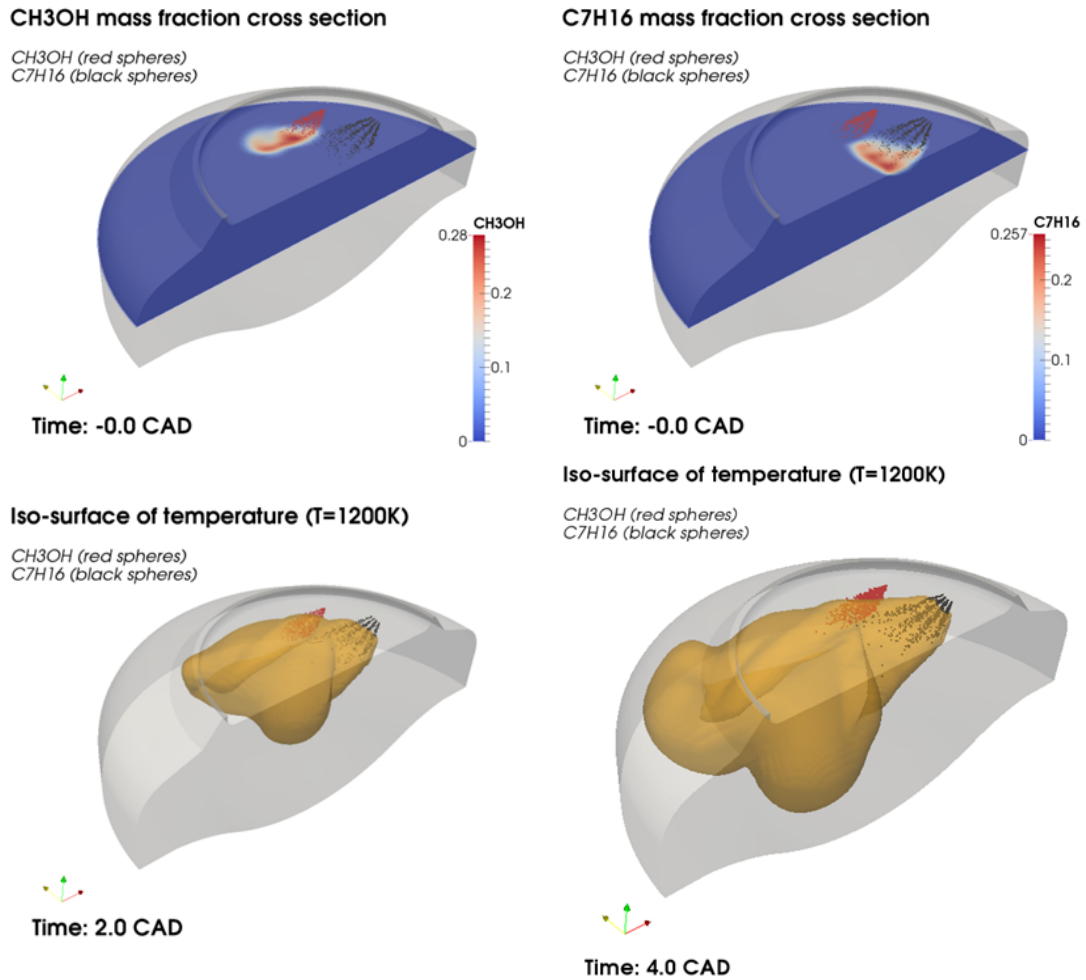
Figure 16: Top figures: Mass fractions at TDC for a dual-fuel CH_3OH (red) and C_7H_16 (black) combustion using a two steps reaction chemical kinetic model. Bottom figures: Iso-surface of temperature (T=1200 K) at 2.0 CAD and 4.0 CAD. Simulation is performed in OpenFOAM.

The computation time is found to be prohibitive even for such a simplified chemical kinetic model, involving only 6 species and 2 reactions, as it took more than a day to complete on 20 cores. Running such a case accurately with a direct integration of the DTU-C2 model which involves alone about 68 species and 665 reactions and an n–heptane model (even if neglecting the turbulence chemistry interaction) is obviously currently out of reach in an industrial framework. State of the art alternatives such a model reduction together with chemistry coordinate mapping or tabulated chemistry are to be explored in the extension of this work package.

24

1.6 Conclusions

The oxidation of methane, ethane, ethanol, propane, and butane have been investigated by tests in a laminar-flow reactor at intermediate temperatures (450–900 K) and high pressures (20–100 bar). The provided data extend the oxidation benchmark at high pressures and intermediate temperatures. A detailed chemical kinetic model was developed with particular attention to the oxidation chemistry at high pressures relevant to engine conditions. The model was evaluated against present data as well as other characteristics data from literature. In general, the model could predict the oxidation properties of aforementioned fuels reasonably well. Models validated against such data can be more confidently used in engineering tools for ignition delay time calculation and tabulation or laminar flame speed calculation as developed in this work package. As observed in a proof of concept, the direct use of such model in multi-fuel CFD simulations is computationally prohibitive and it therefore requires alternatively a mechanism reduction with chemistry coordinate mapping approach or a tabulated approach. These techniques will be explored in the extension of this work package (PART B).

2 Deliverable PART B

2.1 Executive summary

In addition to the findings on detailed chemical kinetic models reported in PART A of this deliverable [66], the present PART B focuses essentially on 3-Dimensional Computational Fluid Dynamics (CFD) simulations. Within the OpenFOAM framework, an advanced mesh handling and dynamic solver developed by POLIMI, initially used in automotive applications, has been enhanced and tailored for large two-stroke marine engine simulations. As shown in Figure 17, the simulations of such engine especially during the scavenging process (charge preparation) requires complex meshes that accounts for valve and piston movements.

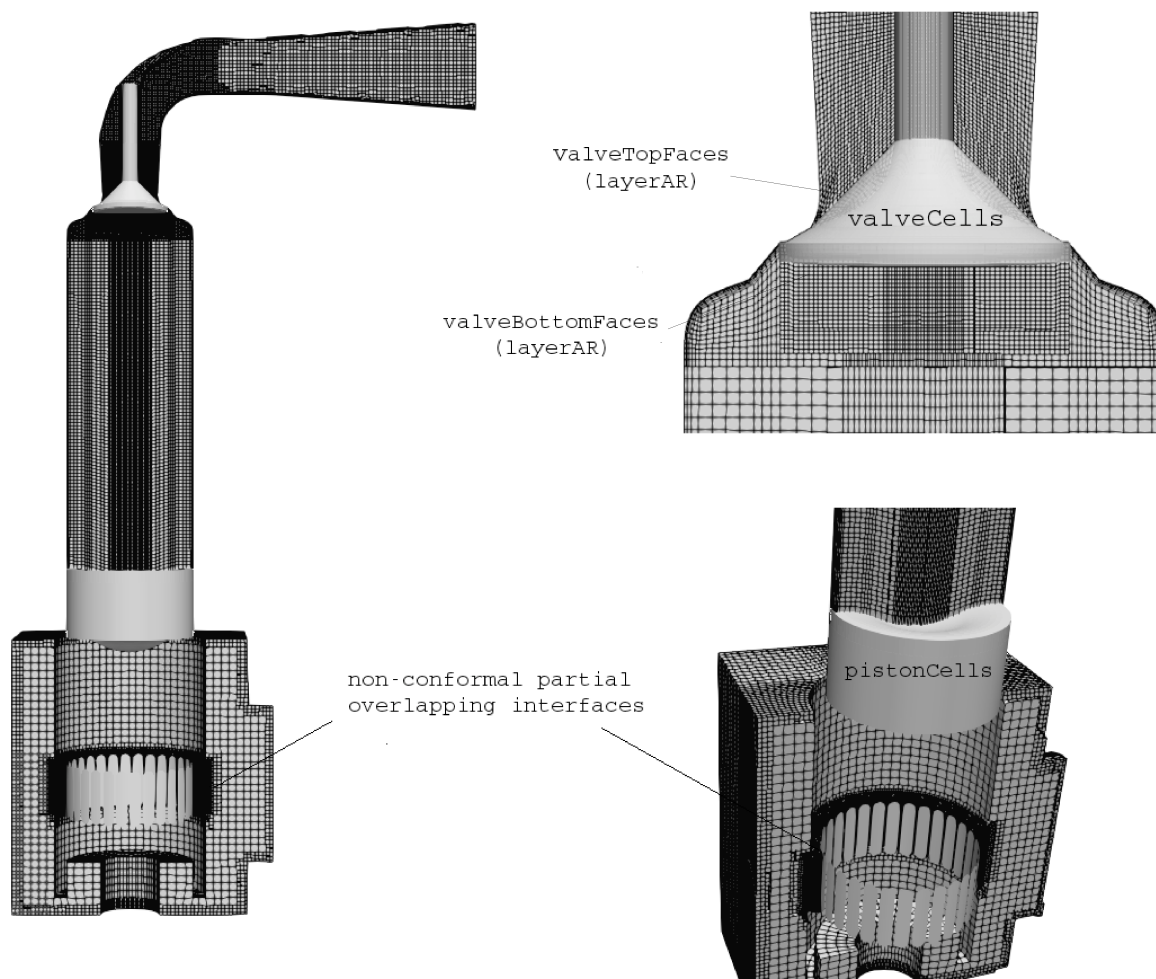Figure 17: Example of mesh definition in the large two-stroke marine engine.

The improvements in the algorithm for dynamic attach/detach of mesh boundaries and in the formulation of a transient solver for compressible turbulent flows as well as others not mentioned here have allowed the correct operation of the combined use of topology modifiers leading to faster and more accurate simulations. These developments

26

and methodology have been validated on a motored cycle and can be used to study the charge preparation prior to the combustion process.

The combustion process modeling using detailed chemical kinetic model has also been the main focus of this work package both in zero- and multi-dimensional CFD. In 3-dimensional CFD simulation in engines, such models, are necessary for having a correct prediction of ignition delay time and flame structure. However to overcome the computational cost of direct integration of large chemical kinetic models, such as the one developed in this work package and reported in PART A of this deliverable, additional modeling is required. Two approaches are evaluated in this report; a direct integration method accelerated by means of cell clustering referred to as Chemistry Coordinate Mapping (CCM) developed by LUND and a tabulated kinetics method in which off-line look-up table developed by POLIMI are used. In both cases, the aim have been to keep enough complexity in the chemical kinetic model so it remains predictive over a relevant range of conditions. In collaboration with work package 2.2 [67], a series of experiments has been performed in a large two-stroke test engine at MDT with the objective to support the validation of the combustion process modeling with high quality data for diesel and multi-fuel operations. The test engine was fitted with three high speed cameras and it was operated on both Diesel and gas fuels. The use of cameras limited the number of Diesel and gas fuel atomizers to one each. Figure 18, presents an example of such validation for a given Diesel operating condition using the two modeling approaches.
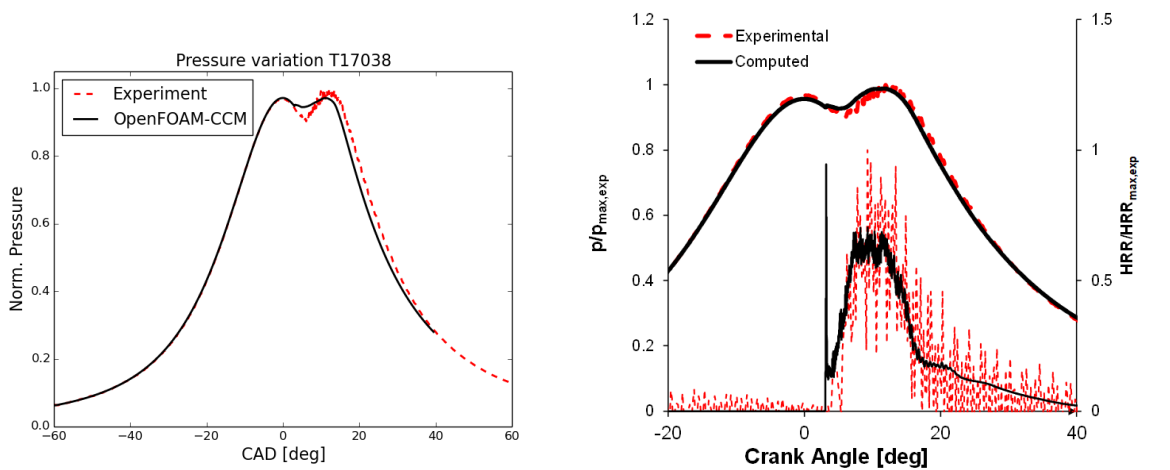
Figure 18: Comparison between computed and experimental data of in-cylinder pressure (and heat release) for diesel combustion modeling using chemistry coordinate mapping (left) and tabulated kinetics (right).

The results obtained in Diesel mode were found very promising for the two approaches. The tabulated kinetics was further applied to dual fuel mode with good results.

In the remaining months of the project, these approaches will be further investigated and evaluated in terms of robustness, accuracy and computational efficiency.

2.2 Introduction

Climate change has become a serious concern nowadays. The main reason of the current changes in the climate is believed to be the high emission of greenhouse gases mainly from human activities. The energy demand has increased exponentially [4] and even though the fuel efficiency improved globally, the CO_2 emission has increased considerably [4]. The steady increase in the global energy demand as well as in the release of carbon dioxide and other harmful pollutants from the combustion of most fossil fuels are the major motivations to seek alternative sources of energy. In a mid-term prospect, fuels which produce less pollutants and CO_2, and have a higher energy efficiency may relieve the environmental problems to some extent. For marine applications, alternative fuels such as Liquefied and Compressed Natural Gas (LNG and CNG), methanol and Liquefied Petroleum Gas (LPG) are currently among the most viable options. In a global transportation system, these fuels might be supplied in various compositions and/or purity which effects should be accounted for. Methane (CH_4) and ethane (C_2H_6) are the major components in LNG and CNG. Neat ethane can also be used as an engine fuel for ships transporting feedstock ethane. Propane (C_3H_8) and butane (C_4H_{10}) are the major component of LPG. Trace amounts of propane and butane can be also found in natural gas. The variations in CH_4, C_2H_6, C_3H_8, and C_4H_{10} fractions can affect the ignition, oxidation, and pollutant formation of the given fuels considerably. Experimental study of the effects of changing fuel in practical conditions are not always economic or even feasible, which emphasizes the role of modelling in design/optimization of engines.

As documented in deliverable D2.4 PART A [66], a high-pressure flow-reactor was used at DTU to investigate the oxidation properties of methane, ethane, ethanol, propane, and butane at high pressures (20–100 bar) and intermediate temperatures (450–900 K). The experiments revealed the onset of fuel oxidation at temperatures starting from 600 K up to 825 K, depending on pressure and fuel-air equivalence ratios. It was found that the oxidation of both methane and ethane starts around 750 K (100 bar, stoichiometric mixture) while propane and butane are oxidized at lower temperatures of 600–700 K (100 bar, stoichiometric mixture). Ethanol is oxidized at 700 K if the pressure is 50 bar.

The data collected from the flow-reactor was used to develop a detailed chemical kinetic model for the combustion of aforementioned fuels at pressures and temperatures relevant to marine engine operating conditions. For instance, Figure 19 shows the gas composition at the flow-reactor outlet for a methane oxygen mixture under stoichiometric conditions for different isotherms. The model reproduces accurately the onset of reaction as well as the relative changes in the fractions of stable components. However, it underpredicts the conversion of methane and oxygen at high temperatures, accompanied by an underprediction of CO_2.
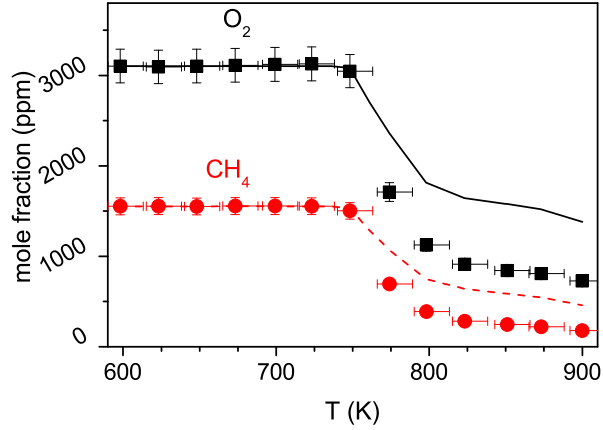
Figure 19: Results for methane under stoichiometric conditions (Φ=1.0) at 100 bar. Symbols mark the experimental results and lines denote the predictions of the developed detailed chemical kinetic model.

The developed model was further evaluated against existing data in literature. Flame speed and ignition delay time predictions were especially evaluated due to their importance for:

- capturing key physics using Computational Fluid Dynamics (CFD) low-dimensional engineering tools.

- performing accurate multi-dimensional CFD calculations.

In general, the model could predict the oxidation properties of aforementioned fuels reasonably well as shown in Figure 20 for methane ignition delay time.
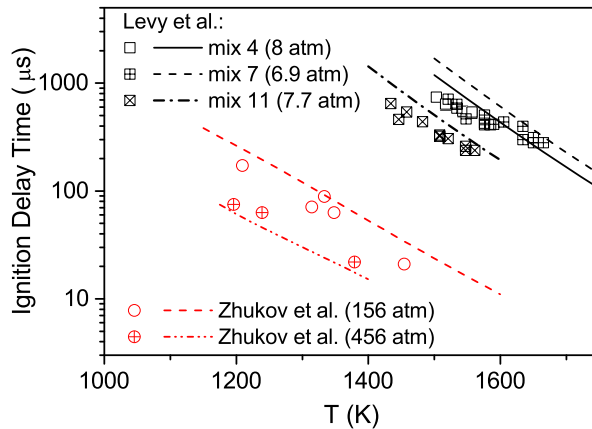
Figure 20: Ignition delay times of CH_4/air (Φ=0.5, from Zhukov et al. [1]) and CH_4/O_2 mixtures (from Levy et al. [2], mix 4: 3.53% CH_4 in N_2, 8 atm, Φ=1.01; mix 7: 4.0% CH_4 in N_2, 6.9 atm, Φ=1.33; mix 11: 1.99% CH_4 + 3.72% CO_2 in N_2, 7.7 atm, Φ=0.32). The simulations are conducted at fixed pressures while the pressure in the experiments fluctuated within $\pm$10%.

This comprehensive evaluation of the model and its application range are described in PART A of this deliverable[66]. The improvement of the model prediction for propane

and butane as well as the evaluation of the model against measured flame data for propane are currently under further investigations.

This detailed chemical kinetic model was then used as the basis of two engineering tools, developed at MDT, that allow a quick evaluation of respectively the ignition delay time and the laminar flame speed of various fuel composition under engine-like conditions. These tools can also be used to create ignition table for example. They were based on the open-source software Cantera [3] and Python programming language.

Using a detailed chemical kinetic models into a multi-dimensional CFD simulation in engine is necessary for having a correct prediction of ignition delay time and flame structure. It is important to notice that the two possible approaches are either the use of direct integration or to generate an off-line look-up table. A proof of concept for direct integration of chemical kinetic models into a multi-dimensional CFD simulation for dual fuel was conducted for a methanol-diesel configuration in [66]. Although OpenFOAM was found to be a very good tool for such studies, it was concluded that direct integration of the developed detailed chemical kinetic model into a multi-dimensional CFD simulation of dual fuel is prohibitive and beyond the reach of industrial application without further reduction. A direct integration of a simplified description of chemistry can be used. Such simple models were expected to fairly well reproduce selected aspects of combustion, e.g. ignition or pollutant emission under a given operating range. Within WP2, MDT proposed to significantly boost the multi-fuel modelling capabilities. First the computation time could be further decreased without reducing the chemical kinetic model dramatically by using an additional strategy such as Chemistry Coordinate Mapping (CCM) developed by Lund University (LUND). Second, the off-line look-up approach referred to as tabulated kinetics developed in the Lib-ICE code by Politecnico Di Milano (POLIMI) is investigated. Finally computational efficiency and accuracy for the charge preparation i.e. scavenging process is critical in such a complex geometry. This aspect is covered in collaboration with POLIMI. These results are documented in this report.

2.3   Objectives

The objective is to develop the numerical tools required to exploit new alternative fuels
in future marine engines. In order to operate efficiently on a larger variety of fuels an
increased understanding of ignition, combustion and emissions formation of those novel
or mixed fuels is required. Numerical tools can provide insight in ignition and emission
formation. Detailed chemical kinetic models evaluated against experimental data at
conditions relevant for marine engines are required to develop such tools. Experimental
measurements will be conducted in a high-pressure flow-reactor facility in DTU Chemical
Engineering to facilitate model development and evaluation (PART A). Within the work
package extension framework (PART B), it is expected that

- POLIMI is to apply and evaluate methods, mesh handling and models initially de-
  veloped for the automotive industry in a large two-stroke marine engine framework.
  Especially the mesh handling and turbulence prediction will be complementary to
  the support of LTH on detailed chemistry.

- LTH will first evaluate the CCM approach in case of multi-fuels combustion in a
  large two-stroke Diesel engine. Then the effect of turbulence chemistry interaction
  will be investigated by means of a pdf approach.

- Investigations by all partners on simulation speed-up techniques are expected as
  well.

2.4 Engine test data

In collaboration with work package 2.2 [67], a series of experiments has been performed in a large two-stroke test engine at MDT. The objectives were to support the current work package with high quality data for model development and calibration for diesel and multi-fuel combustion as well as to investigate new measurement techniques. The test engine was fitted with three high speed cameras as shown in Figure 21 and it was operated on both Diesel and gas fuels.
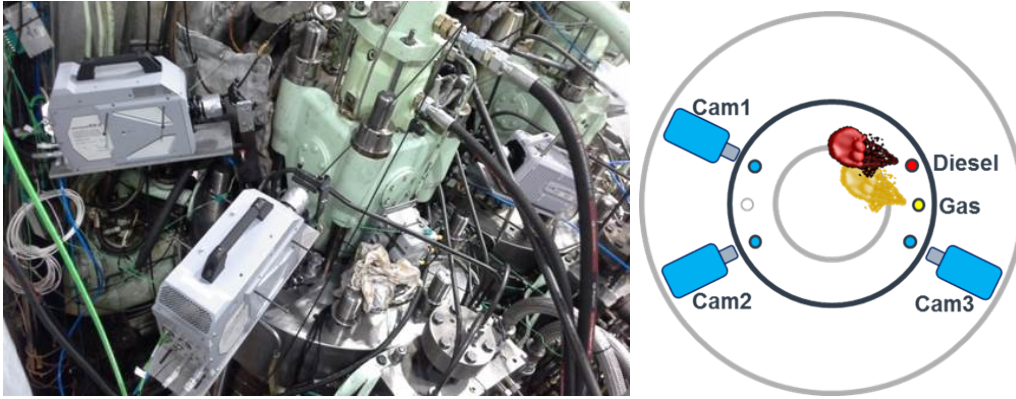

Figure 21: Multiple (x3) high speed cameras mounted on the cylinder cover (left) and schematic showing the camera insert, diesel and gas atomizer in the cylinder (right).

Initial image processing results were presented in [68] and the complete analysis will be documented in deliverable reports D2.5 and D2.6. At this stage of the project, the operating points presented in Table 3 have been used for CFD.

Table 3: Simulated operating points in Diesel and dual-fuel mode

Point	Engine Speed [rpm]	Load	Mode
1	78	-	motored
2	78	low	Diesel
3	111	high	Diesel
4	78	low	Dual-fuel
5	111	high	Dual-fuel

More experimental data, including the image processing, is intended to be used in this work package. The synergy between high quality measurements, state of the art optical diagnostic techniques (in-situ) as well as CFD is believed to provide significant insight for this study on multi-fuel ignition and combustion process.

2.5 Mesh handling and dynamic solvers

2.5.1 Motivations

As evidenced in [69], one of the current bottlenecks limiting CFD code performance in IC engine simulation is related to dynamic mesh handling and in the coupling between the moving mesh strategy and the compressible solver. The aim of this Work Package (WP) was stating its ambition in the context of the following recent and past advances, with particular attention to the optimization of an advanced technique for dynamic mesh handling based on topological changes together with fast and accurate dynamic solvers, to be implemented in a set of dynamic C++ libraries to link to the open-source OpenFOAM CFD code. The resulting framework has been used as a tool for the simulation of the physical processes occurring in the large bore two-stroke marine engines. An already existing methodology [70–73] developed at POLIMI has been extended and generalized to perform fast and reliable parallel simulations in such engines. This methodology and the associated libraries are currently validated by weekly regression tests and daily checks and are maintained onto two on-line GIT repositories. These repositories allow being aligned to OpenFOAM releases by OpenCFD and to the OpenFOAM-dev version by the OpenFOAM Foundation.

2.5.2 Code development

Among all the approaches available for the mesh handling for scavenging process simulation, a strategy based on block-structured grids (to discretize the cylinder region, the exhaust duct and the cylinder ports respectively) sharing non conformal Arbitrary Mesh Interfaces (`AMI`) and Arbitrary Coupled Mesh Interfaces (`ACMI`) has been chosen. The strategy, shown in Figure 22, has been successfully combined with the dynamic addition/removal (`layerAR`) of layers of hexahedral cells occurring during the piston and the valve motion and with the capability to attach and detach mesh regions on-the-fly. During the simulation, a prescribed motion is set for the piston and the valve boundaries, which rigidly translate. Almost no cell deformation and remeshing are present in the scavenging simulation therefore mesh quality away from the boundaries is fully preserved and it can still be controlled near moving walls. As a result, a single mesh is moved by the automatic mesh motion during the simulation of the whole scavenging process.
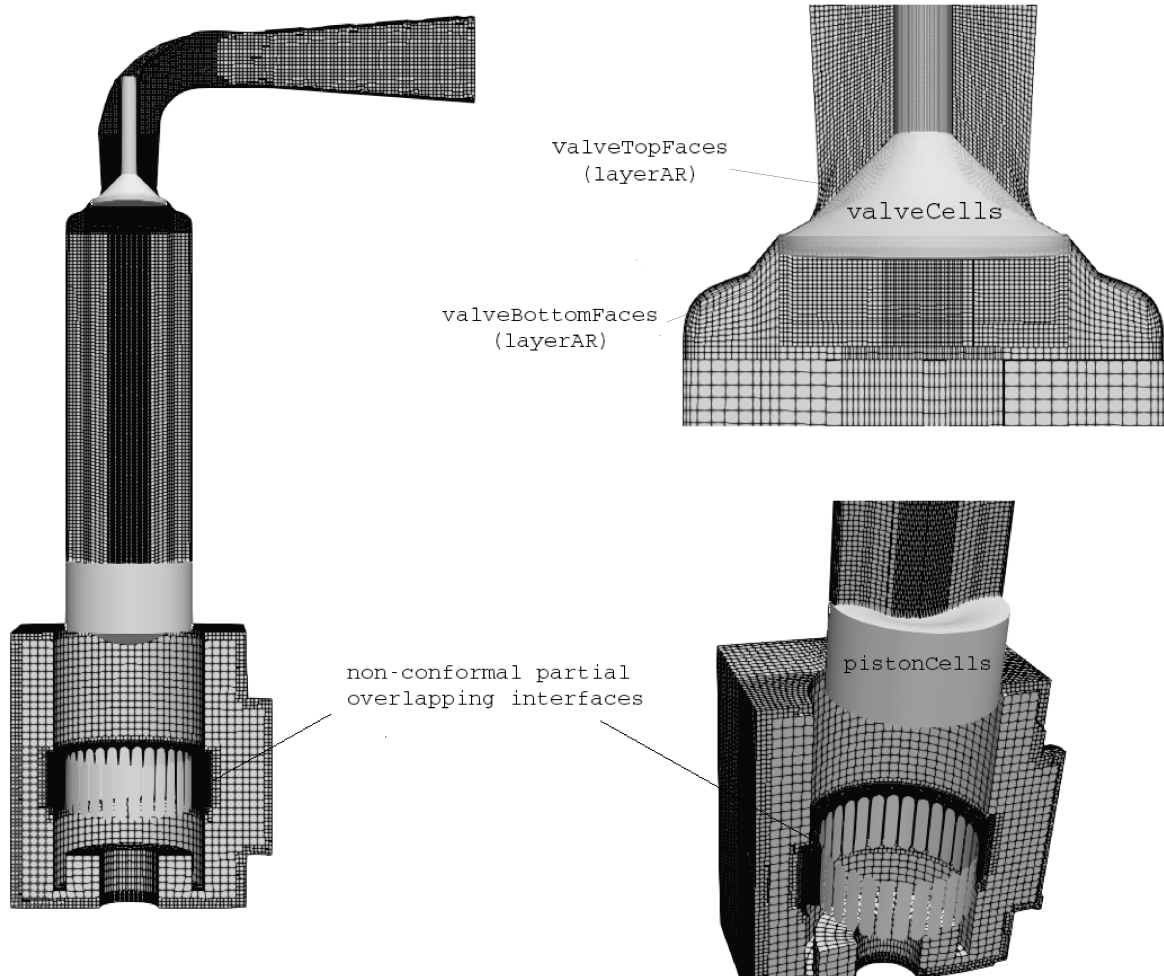
Figure 22: Example of mesh definition in the large two-stroke marine engine.

The described strategy, initially implemented at POLIMI and described in [70–72] has been applied, optimized, extended and improved to simulate of large-bore two-stroke marine engines. In this work package, some significant enhancements have been implemented as extensions to the already existing code:

- the robustness of the algorithm for dynamic attach/detach of mesh boundaries has been improved (Figure 23), as well as the conservativeness of the solver in multiple-region problems;

- extensions to the class for dynamic addition and removal of cell layers have been employed to ensure a correct operation of the dynamic layering technique in combination of the Arbitrary Coupled Mesh Interfaces (ACMI), that are used to model the partial overlap between the piston and the intake ports during scavenging.

- An improved formulation of a transient solver for compressible viscous and turbulent flows, based on a merged PISO-SIMPLE algorithm has been updated to work with the latest OpenFOAM releases. Specific modifications/improvements to the solver have been employed during this project, to reduce the vector operations and to enforce

34

conservation of interface fluxes when dynamic addition of cell layers is applied. As a result, a further speed-up of the code has been obtained;

- code developments for post-processing at runtime (`functionObjects`);

- support for `crankNicolson` second order time scheme with dynamic layering.
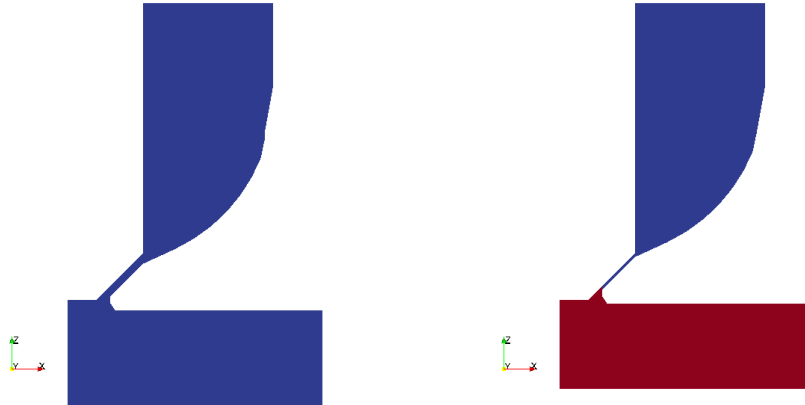

Figure 23: Example of attach/detach of the exhaust valve during a full-cycle simulation.

The employed modifications have allowed the correct operation of the combined use of the topology modifiers, which is not currently supported by OpenFOAM releases. The advantages of the work carried out have been proved to be multiple:

- the approach allows to preserve the initial mesh quality (skewness, non-orthogonality and aspect ratio) during the whole engine cycle (or, more in general, during all the simulation), since grids at different time steps differs only for layers of fully orthogonal hexahedral cells, favouring a very fast convergence of the solution over a multi-block grid;

- during cylinder compression, as the piston is moving towards the Top Dead Center (TDC), the number of cells decreases together with the overall computational load; if this is combined to an efficient algorithm for domain decomposition providing acceptable load balancing.

In order to simulate a complete cycle, it has been combined with a closed cycle simulation strategy (closed valve and closed ports). The overall mesh motion strategy adopted and the turbulence modeling used were the same for two sets of simulations:

1. one single mesh was used from the beginning of the scavenging until the exhaust valve closure (see Fig. 22). Dynamic addition of cell layers was applied during piston and valve motion.

2. a mesh strategy based on point stretching and/or mesh-to-mesh interpolation has been used for the closed-cycle simulation such in [74].

2.6 Simulations of charge preparation

In the following, the validation of the modeling strategy is performed using the motored cycle simulation from Table 3. It is supported by the comparison between the experimental and the calculated in-cylinder pressure trace. Figure 24 shows a very good agreement between the in-cylinder pressure simulated and measured for the complete cycle.
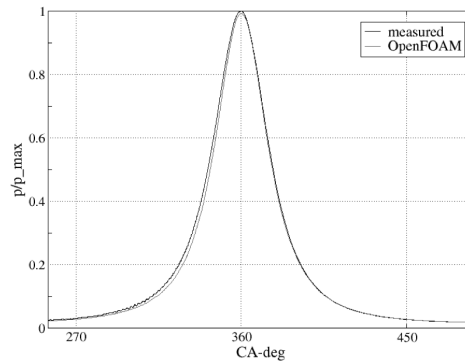

Figure 24: In-cylinder pressure trace of the full-cycle simulation of the two-stroke large bore engine employed at MAN Diesel & Turbo .

In Figure 25-26, the contour plot of the instantaneous flow field is reported at different crank angles. The following figures are referred to full-cycle simulations of engine operating under motored run conditions.
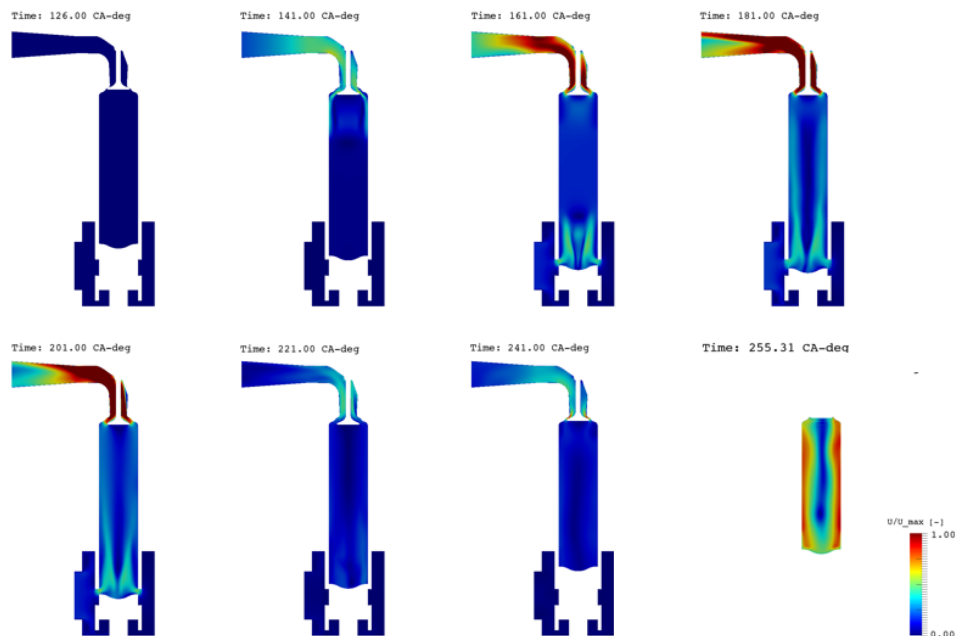

Figure 25: Simulation of the scavenging process. One single mesh is used from the intake port opening up to the Exhaust Valve Closure (EVC).
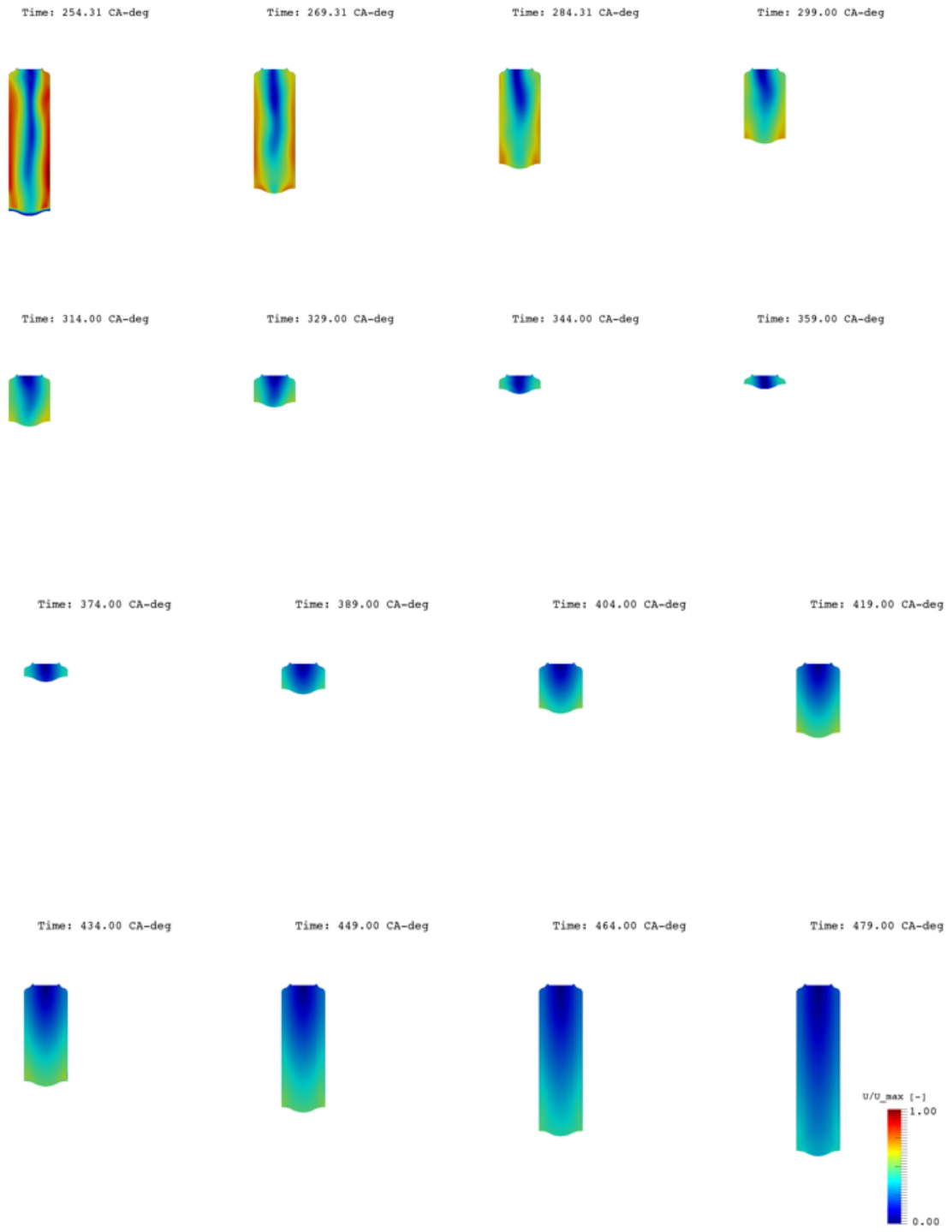
Figure 26: Simulation of the closed cycle (compression and expansion). Multiple grids are used.

This modeling strategy can be applied to generate the initial conditions i.e. charge preparation for all cases reported in Table 3.

2.7 Simulations of combustion process

2.7.1 Modeling strategies

Chemistry coordinate mapping

The idea behind Chemistry Coordinate Mapping (CCM) is to cluster the cells in CFD domain with respect to their composition and thermodynamic state and map them to chemistry state and compute the reaction rate source terms in this a low dimensional manifold. These source terms then are mapped back to the physical coordinate in which the transport equations are solved. To cluster the cells in physical space domain, three parameters are chosen; temperature, elemental mass fraction of hydrogen atom, and scalar dissipation rate. In addition to these three parameter, the mass fraction of fuel and N2 are also included. The model accepts as many parameters as the user requires to build the chemistry state manifolds. The reasons behind this selection of chemistry coordinate dimensions are presented in the original paper with details [75, 76]. Temperature is used as a progress variable, elemental mass fraction of hydrogen atom takes into account the differential diffusivity and scalar dissipation rate reflects on turbulent mixing. After clustering the cells into the chemistry coordinate, the chemistry is solved based on the fractional step methods with smaller time step compared with that of the flow. Then the reaction source terms are mapped back to the CFD domain and for the second fractional step for solving flow transport equations. Figure 27 shows the region of the CFD domain involved in the reaction at three different crank angle degrees. The cluster of the grid cells which is growing by the crank angle degree represents the active cells that are mapped into the chemistry coordinate. The number of cells in the CFD is around 650000 while the number of zones in the chemistry coordinate is below 10000 cells, representing an speed up factor of around 65.
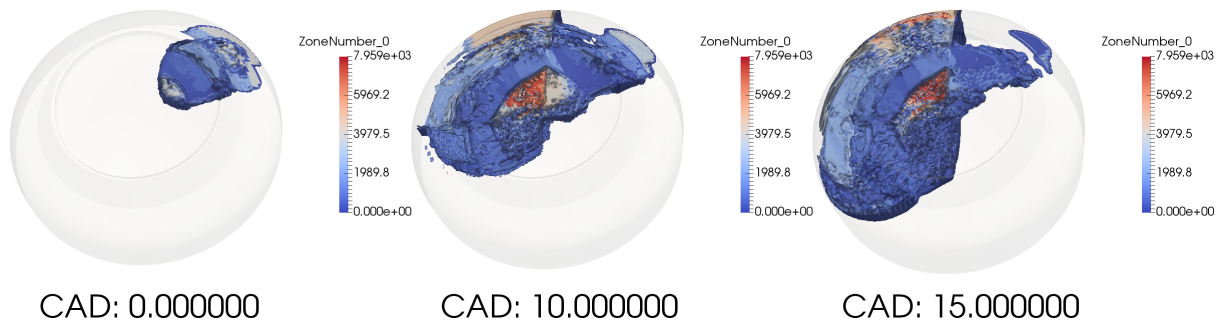

Figure 27: The regions of the CFD domain involved in the reaction at three different crank angle degrees.

For what concerns the chemical kinetics, Diesel fuel is assumed to be n-dodecane while the IDEA surrogate properties were used to describe its behaviour (density, vapour pressure, surface tension, heat capacity, viscosity) in the liquid phase. A skeletal mechanism with 54 species and 269 reactions for n-dodecane combustion was used in these simulations [77].

Tabulated kinetics

In the tabulated kinetics approach, reaction rates and chemical composition are stored in a lookup table which is generated from a chemical mechanism and the assumption of a certain flame structure like a perfectly stirred reactor or laminar diffusion flame. Figure 28(a) summarizes the way chemistry is tabulated in the proposed approach. The user specifies a chemical mechanism and a range of initial conditions for calculations of a homogeneous constant-pressure reactor in terms of:

- Mixture fraction Z

- Ambient pressure p

- Initial reactor temperature T_u

- Residual gas fraction, or Exhaust Gas Recirculation (EGR)

Based on such quantities, initial chemical composition is computed and the reactor calculation is started. For any specified condition, chemical species equations are solved according to:

$$\frac{dY_i}{dt} = \omega\left(T, p, Y_1, ..., Y_n\right) \tag{3}$$

with reactor temperature T computed directly from the initial enthalpy value. After every time step, the progress variable C is evaluated together with the computation of the chemical composition by means of the virtual species approach. The progress variable C is equal to the heat released by combustion, computed as the difference between the current and the initial value of the reactor formation enthalpy, also known as h_{298}. At the end of each reactor calculation, progress variable reaction rates, chemical composition, minimum and maximum progress variable values (C_{min} and C_{max}) are stored as function of the discrete values of the normalized progress variable c, specified by the user:

$$c = \frac{(C - C_{min})}{(C_{max} - C_{min})} \tag{4}$$

To avoid excessive memory consumption, only seven virtual species are tabulated for any value of the progress variable c. Their mass fractions are computed in order to preserve the main thermochemical properties of the full set used in the detailed mechanism. The table also includes the mass fractions of chemical species which are of interest for the user (Y_o in Figure 28(a)), either for post-processing purpose or because they are relevant for the formation of the main pollutants required for the related sub-models.
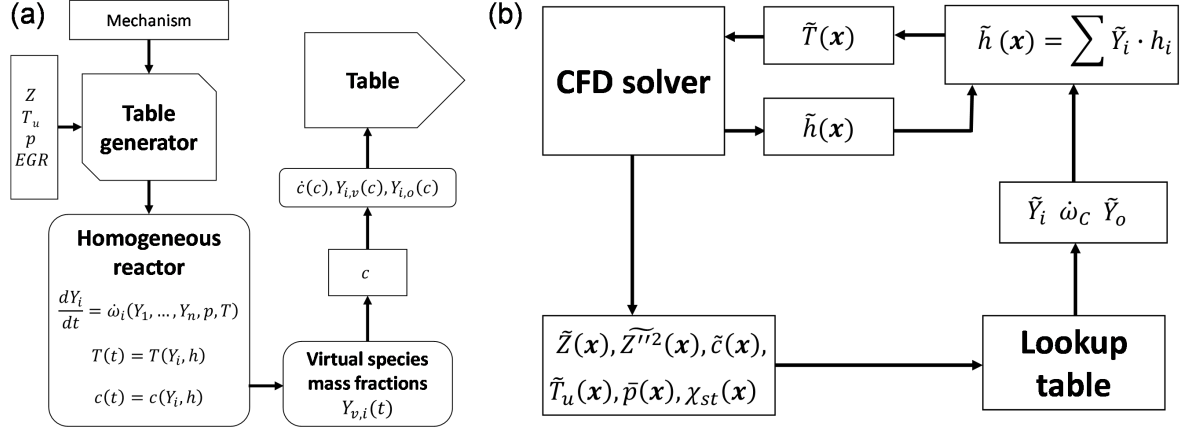
Figure 28: (a) Generation of the chemistry table based on the homogeneous reactor assumption; (b) Operation of combustion models based on tabulated kinetics.

In this work, the homogeneous reactor table is directly employed in the CFD solver (see Figure 28(b)), directly providing reaction rates and chemical composition with the so-called "tabulated well-mixed" (TWM) approach. Other approaches including turbulence-chemistry interaction are also possible including presumed PDF or tabulated flamelet progress variable. Such models will be tested hereinafter. To model dual-fuel combustion, a simplified approach was developed where ignition is governed by local thermodynamic conditions and progress variable diffusion. In this way, it is possible to use separate tables for any fuel without the need to use too complex mechanisms. Air is assumed to be equally distributed between the two fuels and this makes possible to consider only the global cell mixture fraction for the computation of reaction rates and chemical composition. Both progress variable reaction rate and chemical composition are computed as the weighted average of the corresponding mixture fraction values for the two fuels. Figure 29 summarizes how tabulated kinetics was employed for the simulation of dual-fuel combustion: in any cell there is only one progress variable which makes possible to account for both the effects of local conditions and flame propagation (due to progress variable diffusion) on the ignition process.
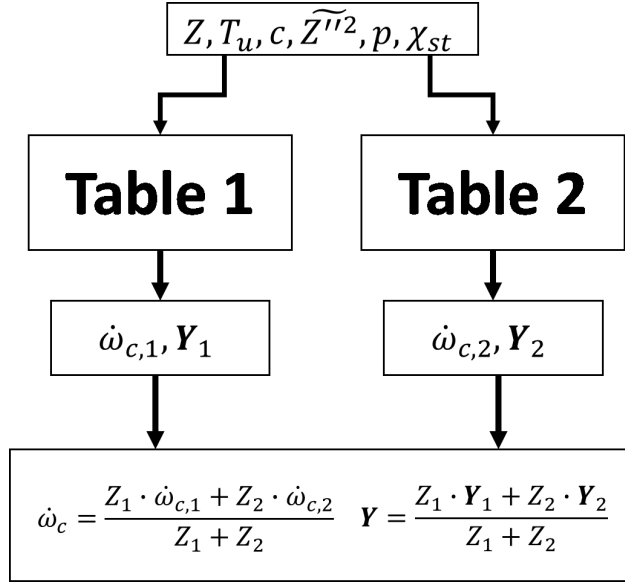
Figure 29: Tabulated kinetics for dual fuel combustion modeling.

In the present work, natural gas is assumed to be methane and its oxidation is modeled using the GRI mechanism with 53 chemical species. Due to the very similar cetane number, Diesel fuel is assumed to be n-heptane and the LLNL mechanism with 159 species was used. The IDEA surrogate properties were adopted to describe the Diesel fuel spray behaviour.

2.7.2 Modeling Diesel mode

Mesh and boundary conditions

Simulations were carried out for part of compression and combustion phases. Start of the simulation was set at 60 CAD BTDC and initial conditions in terms of in-cylinder pressure, temperature, velocity field and chemical composition were provided by MDT and come from 1D and 0D calculations as well as from measurements. The computational mesh represents the full combustion chamber and was provided by MDT. Mesh motion is handled by deforming the grid in the cylinder and keeping it fixed inside the cylinder head region where the spray evolves. This allows a proper description of the spray evolution and fuel-air mixing process. Figure 30 reports the computational mesh at -60 CAD (start of the simulation) and at TDC.
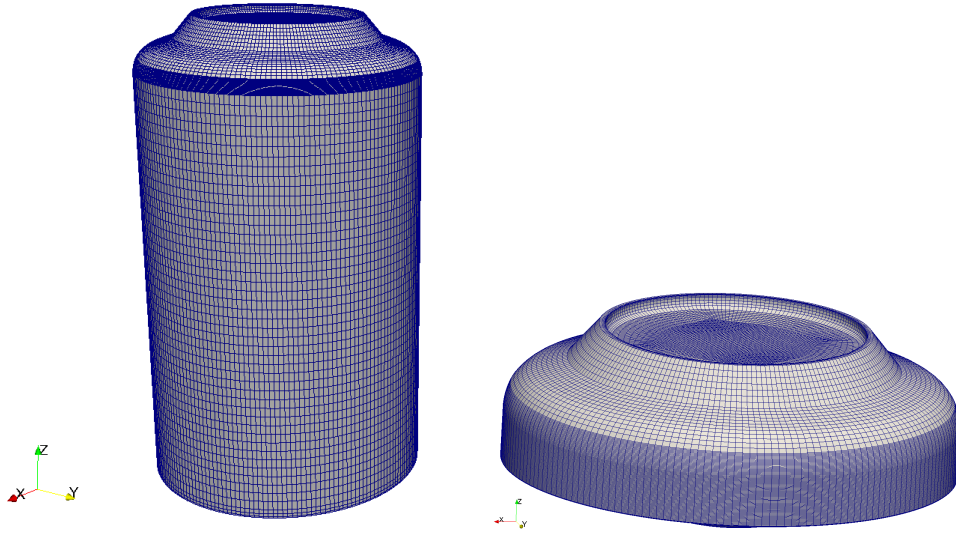
Figure 30: Computational mesh at -60 CAD (left) and TDC (right).

Chemistry coordinate mapping

A good agreement was achieved between the predicted pressure trace in the cylinder and the measured one as shown in Figures 31.
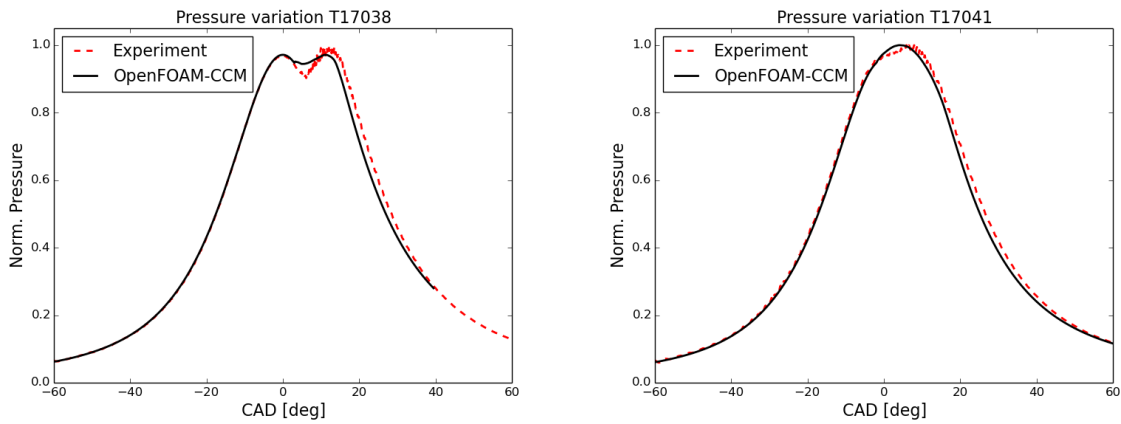

Figure 31: Comparison between computed and experimental data of in-cylinder pressure for the simulated operating points 2 and 3 (Table 3).

Tabulated kinetics

First, tabulated kinetics was assessed with conventional Diesel combustion and Table 3 reports the simulated operating points which are characterized by different loads and speeds. Figure 32 reports a comparison between computed and experimental in-cylinder pressure and heat release rate profiles. The adopted combustion model correctly captures both location and magnitude of in-cylinder peak pressure which is slightly overestimated

(mainly for point 3 condition) due to the lack of turbulence-chemistry interaction. Moreover, for both the simulations the consistency with respect with energy conservation was also verified: at least 99.5% of the fuel lower heating value was released. The consistency of the results achieved on conventional Diesel combustion represents a fundamental pre-requisite for a successful dual-fuel combustion process simulation.

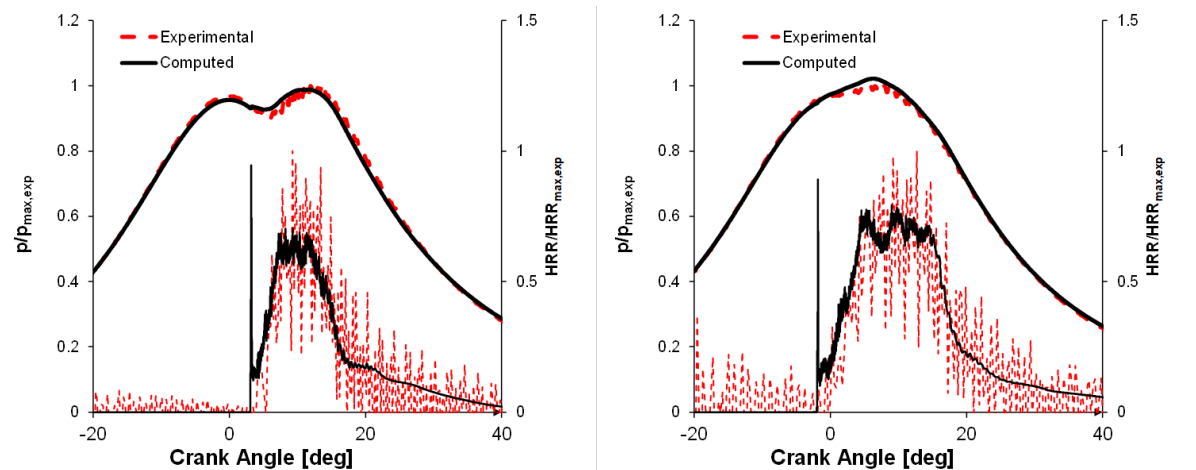Figure 32: Validation of the combustion model with tabulated kinetics for conventional Diesel combustion for the simulated operating points 2 and 3 (Table 3).

For the sake of completeness, Figures 33-34 report details of the mixture fraction and temperature fields during the conventional Diesel combustion process.
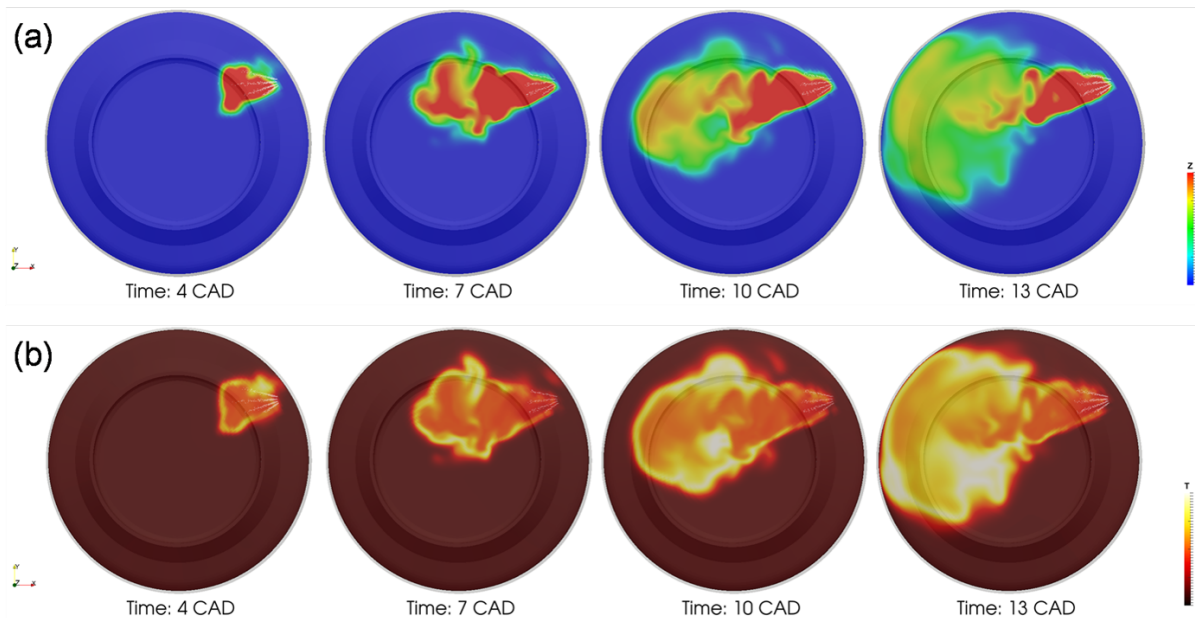

Figure 33: (a) mixture fraction and (b) temperature evolution for the simulated operating point 2 (Table 3).
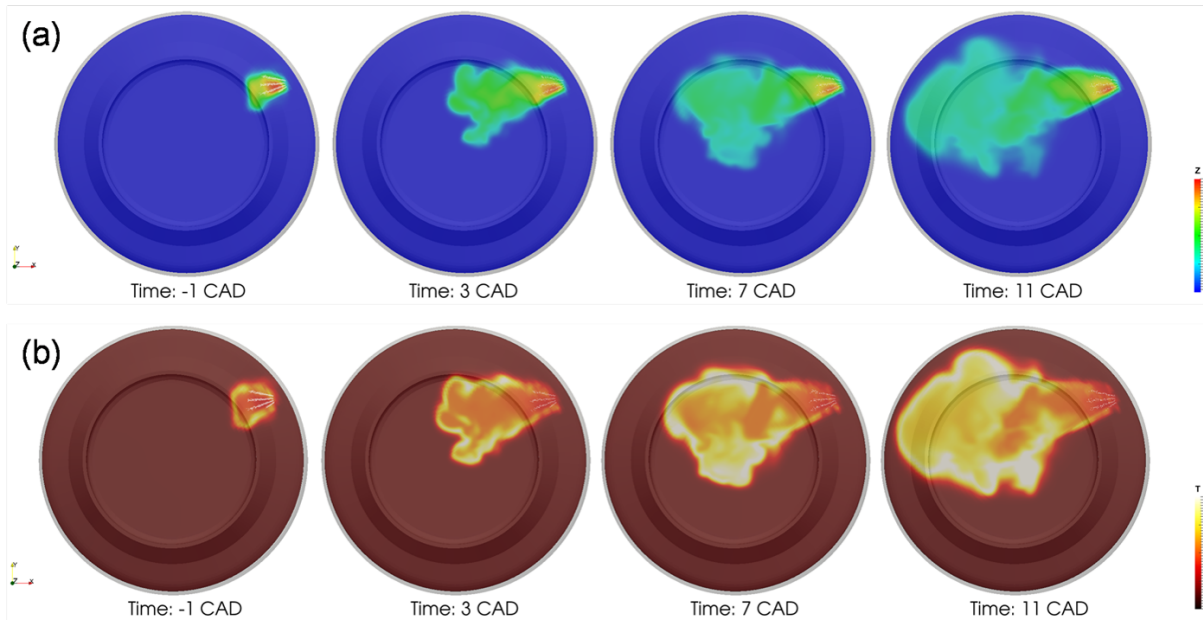
Figure 34: (a) mixture fraction and (b) temperature evolution for the simulated operating point 3 (Table 3).

2.7.3 Modeling dual fuel mode

Mesh and boundary conditions

Simulations were carried out for compression and combustion phases. Start of the simulation was set at 60 CAD BTDC and initial conditions in terms of in-cylinder pressure, temperature, velocity field and chemical composition were provided by MDT and come from 1D and 0D calculations. The computational mesh represents the full combustion chamber and was provided by MDT. Figure 35 shows that the mesh also includes the last part of the natural gas injector geometry. To include such details the grid was generated by suitable scripts combining the two mesh generators available in OpenFOAM: blockMesh and snappyHexMesh. During motion, layers of cells are added above the piston, making possible to keep an almost constant mesh resolution in the combustion chamber region which is important for a correct prediction of the air-fuel mixing process. Mesh size is 800000 cells at 60 BTDC which is reduced to approximately 20000 at TDC.
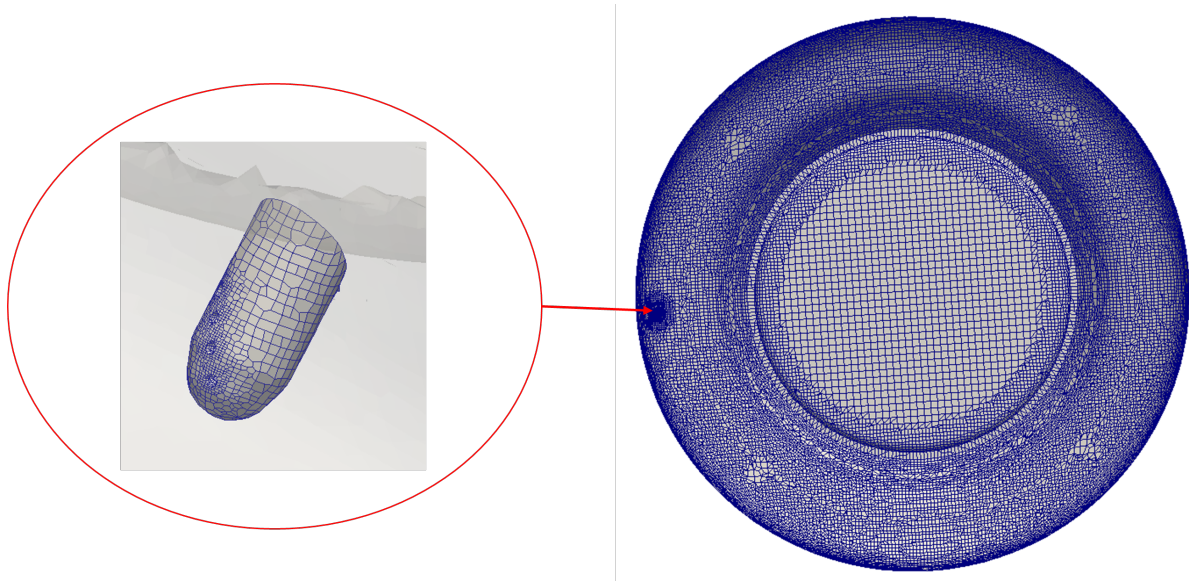
Figure 35: Combustion chamber computational mesh at TDC.

For all dual-fuel conditions, natural gas is injected after a pilot injection of Diesel fuel for better flame visualization. Also because of the optical setup, the engine operates with only one injector for both Diesel and natural gas, respectively.

Tabulated kinetics

Simulation of the dual-fuel combustion process were performed considering two different operating points which are characterized by different speeds and load, as reported in Table 3.

Figure 36 reports a comparison between computed and experimental data of in-cylinder pressure trace annd heat release rate profiles for the dual fuel combustion cases. It is possible to see that the combustion process is rather well predicted. The profile of heat release rate can be divided into two phases: the first is characterized by ignition and combustion of the Diesel fuel. In the second phase there is natural gas combustion.

Figures 37-38 report details of the fuel-air mixing and combustion process for both the simulated operating conditions with dual-fuel combustion. The distribution off the mixture fraction is illustrated in Figures 37(a)-38(a) where it is possible to see that liquid fuel evaporation is followed by gas injection. Temperature distribution is shown in Figures 37(b)-38(b): after Diesel ignition, combustion of natural gas mainly starts due to diffusion of diesel burnt products towards the natural gas fuel jet.
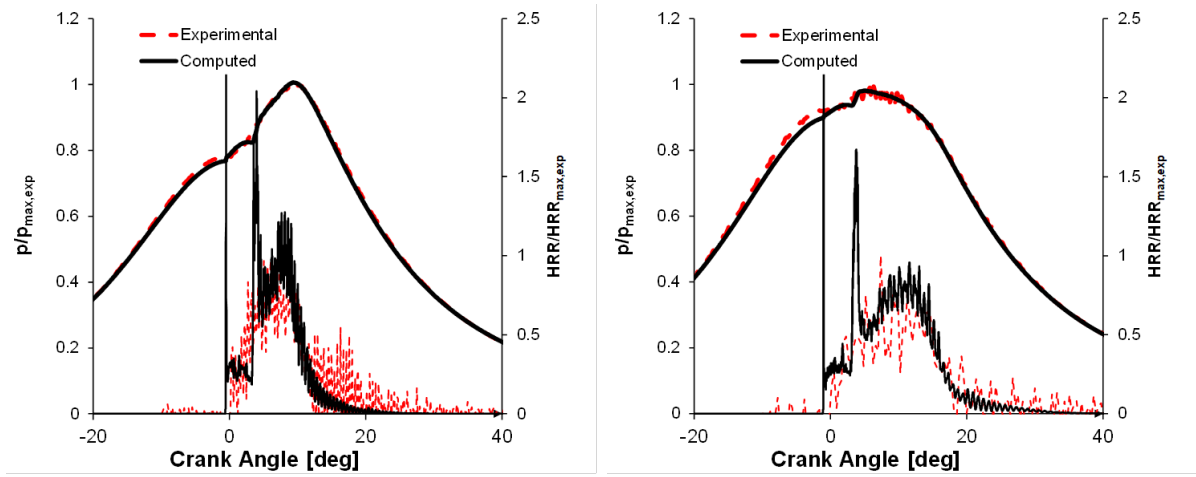
Figure 36: Validation of the combustion model with tabulated kinetics for dual-fuel combustion process for the simulated operating points 4 and 5 (Table 3).
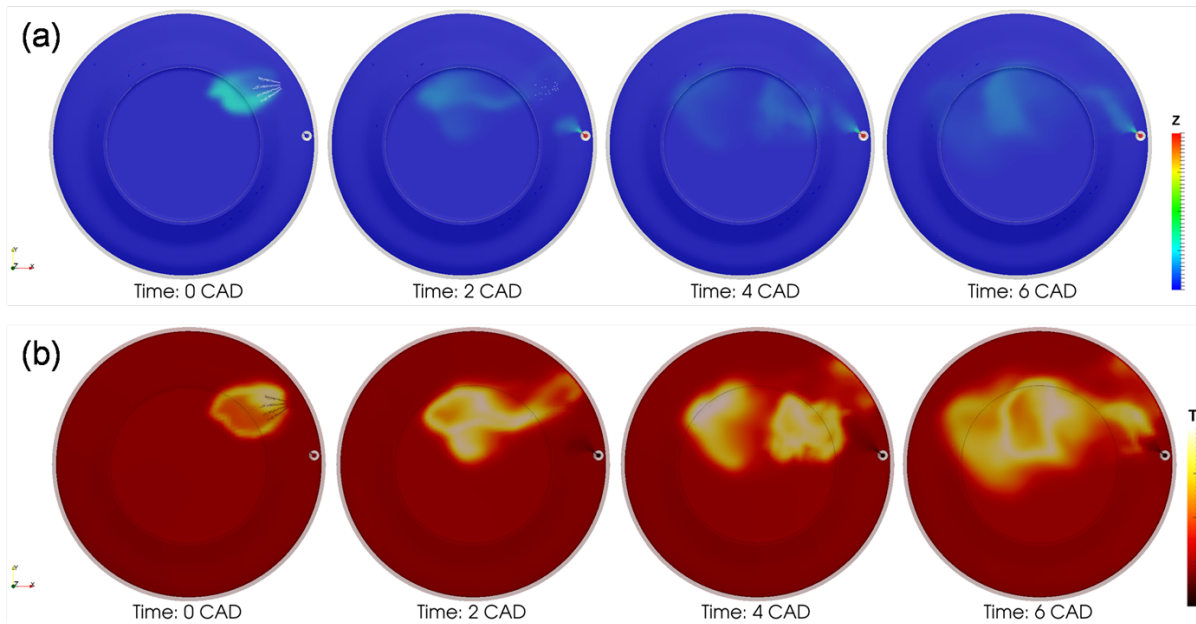

Figure 37: (a) mixture fraction and (b) temperature evolution for the simulated operating point 4 (Table 3).
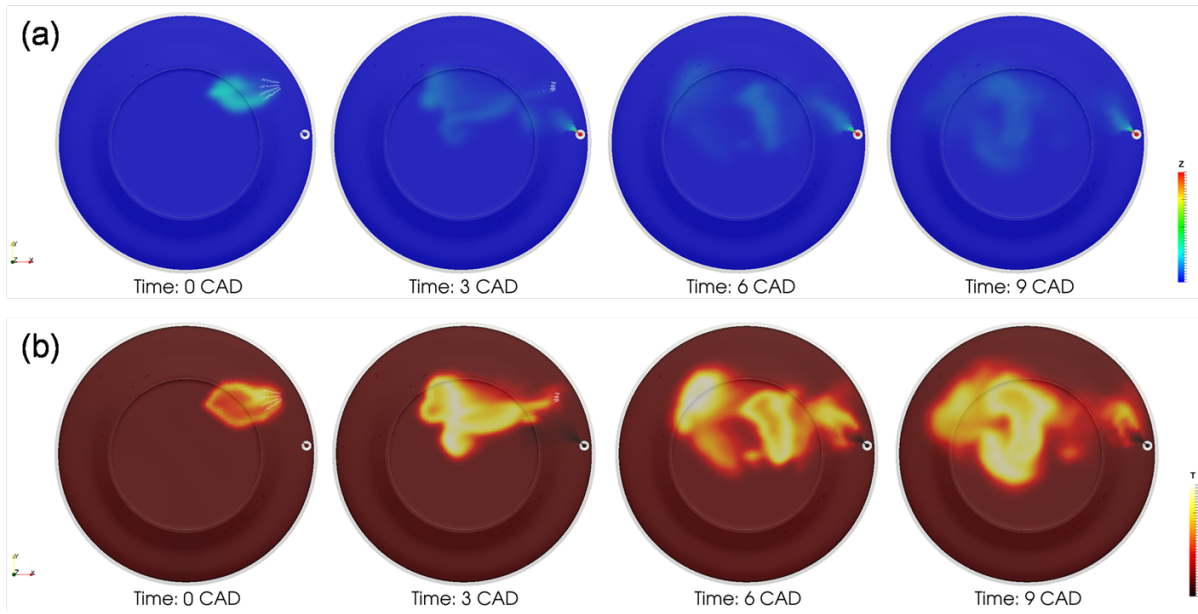
Figure 38: (a) mixture fraction and (b) temperature evolution for the simulated operating point 5 (Table 3).

2.8 Current development

The extension of HERCULES-2 project to october 2018 will allow us to pursue the work presented in this report further. These results will be reported in the final HERCULES-2 report. After a successful calibration and setup against reference Diesel cases in large two stroke marine engine, the work is focusing on multi-fuel combustion i.e methane and Diesel pilot. A new set of geometries as well as boundary conditions for a selected set of experimentally measured cases is being prepared at MAN Diesel & Turbo . In the remaining 6 months of the project:

- the chemistry mechanism for dual-fuel will be evaluated with the CCM approach

- the effect of turbulence-chemistry interaction will be investigated

- additional experimental optical data will used to evaluate the combustion CFD simulations.

2.9   Conclusions

In addition to the findings reported in PART A [66], the second part (PART B) of this work package "Modeling of multi-fuel ignition" focused essentially on CFD calculations and their performance. Within the OpenFOAM framework, an advanced mesh handling and dynamic solver, initially used in automotive applications, has been enhanced and tailored for large two-stroke marine engine. The new methodology derived allowed to perform fast and accurate simulation of the charge preparation which is an important aspect of complete cycle simulation. The combustion process modeling intend to make use of detailed detailed chemical kinetic model for dual-fuel applications, following the work carried out in PART A [66]. Two modeling approaches have been investigated. First, a tabulated kinetics approach with off-line generated tabulation was investigated. The results obtained both in Diesel and dual-fuel modes were promising in terms of accuracy and computational cost. Further investigations and validation are necessary in more practical engine configurations. Second, a direct integration of the chemistry accelerated by the chemistry coordinate mapping approach. The method showed also promising results in Diesel mode both in terms of accuracy and computational cost with respect to non clustered approach. Further investigations in dual-fuel mode as well as on the effect of turbulence chemistry interaction will be carried out in the remaining months of the project. In order for these two combustion modeling approaches to perform accurately, it is important to highlight the need of detailed detailed chemical kinetic, well validated and well documented within the range of engine operating conditions, as covered in PART A [66] which illustrate the completeness of the project.

References

[1] V P Zhukov, V A Sechenov, and A.Yu. Starikovskii. "Spontaneous Ignition of Methane-Air Mixtures in a Wide Range of Pressures". In: *Combust., Explos. Shock Waves* 39.5 (2003), pp. 487–495.

[2] Y Levy, E Olchanski, V Sherbaurn, V Erenburg, and A Burcat. "Shock-tube ignition study of methane in air and recirculating gases mixtures". In: *J. Propul. Power* 22.3 (2006), pp. 669–676.

[3] David G. Goodwin, Harry K. Moffat, and Raymond L. Speth. *Cantera: An Object-oriented Software Toolkit for Chemical Kinetics, Thermodynamics, and Transport Processes.* http://www.cantera.org. Version 2.3.0. 2017.

[4] International Energy Agency. *CO_2 emissions from fuel combustion (2013 Edition).* International Energy Agency, 2013.

[5] Katharina Kohse-Höinghaus, Patrick Oßwald, Terrill A Cool, Tina Kasper, Nils Hansen, Fei Qi, Charles K Westbrook, and Phillip R Westmoreland. "Biofuel combustion chemistry: from ethanol to biodiesel". In: *Angew. Chem., Int. Ed.* 49.21 (2010), pp. 3572–3597.

[6] Christian Lund Rasmussen, Jorn Hansen, Paul Marshall, and Peter Glarborg. "Experimental measurements and kinetic modeling of $CO/H_2/O_2/NO$, conversion at high pressure". In: *Int. J. Chem. Kinet.* 40.8 (2008), pp. 454–480.

[7] Christian Lund Rasmussen, Jon Geest Jakobsen, and Peter Glarborg. "Experimental Measurements and Kinetic Modeling of CH_4/O_2 and $CH_4/C_2H_6/O_2$ Conversion at High Pressure". In: *Int. J. Chem. Kinet.* 40.12 (2008), pp. 778–807.

[8] Gregory P Smith, David M Golden, Michael Frenklach, Nigel W Moriarty, Boris Eiteneer, Mikhail Goldenberg, C Thomas Bowman, Ronald K Hanson, Soonho Song, Jr. William C. Gardiner, Vitali V Lissianski, and Zhiwei Qin. *GRI-Mech Version 3.0.* 1999. URL: http://combustion.berkeley.edu/gri_mech/.

[9] Eric L Petersen, Danielle M Kalitan, Stefanie Simmons, Gilles Bourque, Henry J Curran, and John M Simmie. "Methane/propane oxidation at high pressures: Experimental and detailed chemical kinetic modeling". In: *Proc. Combust. Inst.* 31.1 (2007), pp. 447–454.

[10] F H V Coppens, J De Ruyck, and A A Konnov. "The effects of composition on burning velocity and nitric oxide formation in laminar premixed flames of $CH_4 + H_2 + O_2 + N_2$". In: *Combust. Flame* 149.4 (2007), pp. 409–417.

[11] Hanfeng Jin, Alberto Cuoci, Alessio Frassoldati, Tiziano Faravelli, Yizun Wang, Yuyang Li, and Fei Qi. "Experimental and kinetic modeling study of PAH formation in methane coflow diffusion flames doped with n-butanol". In: *Combust. Flame* 161.3 (2014), pp. 657–670.

[12] J Huang, P G Hill, W K Bushe, and S R Munshi. "Shock-tube study of methane ignition under engine-relevant conditions: Experiments and modeling". In: *Combust. Flame* 136.1-2 (2004), pp. 25–42.

[13] Hilal El Merhubi, Alan Kéromnès, Gianni Catalano, Benoîte Lefort, and Luis Le Moyne. "A high pressure experimental and numerical study of methane ignition". In: *Fuel* 177 (2016), pp. 164–172.

[14] D F Davidson and R K Hanson. *Fundamental Kinetics Database Utilizing Shock Tube Measurements, Volume 1: Ignition Delay Time Measurements*. Internal report. 2005.

[15] James A Miller, Michael J Pilling, and Jürgen Troe. "Unravelling combustion mechanisms through a quantitative understanding of elementary reactions". In: *Proc. Combust. Inst.* 30.1 (2005), pp. 43–88.

[16] Christian Lund Rasmussen, Anja Egede Rasmussen, and Peter Glarborg. "Sensitizing effects of NO_x on CH_4 oxidation at high pressure". In: *Combust. Flame* 154.3 (2008), pp. 529–545.

[17] Jorge Gimenez Lopez, Christian Lund Rasmussen, Maria U Alzueta, Yide Gao, Paul Marshall, and Peter Glarborg. "Experimental and kinetic modeling study of C_2H_4 oxidation at high pressure". In: *Proc. Combust. Inst.* 32 (2009), pp. 367–375.

[18] V Aranda, J M Christensen, M U Alzueta, P Glarborg, S Gersen, Y Gao, and P Marshall. "Experimental and Kinetic Modeling Study of Methanol Ignition and Oxidation at High Pressure". In: *Int. J. Chem. Kinet.* 45.5 (2013), pp. 283–294.

[19] J.G. Lopez, C.L. Rasmussen, H. Hashemi, M.U. Alzueta, Y. Gao, P. Marshall, C.F. Goldsmith, and P. Glarborg. "Experimental and Kinetic Modeling Study of C_2H_2 Oxidation at High Pressure". In: *Int. J. Chem. Kinet.* 48.11 (2016), pp. 724–738.

[20] Hamid Hashemi, Jakob M Christensen, Sander Gersen, Howard Levinsky, Stephen J Klippenstein, and Peter Glarborg. "High-Pressure Oxidation of Methane". In: *Combust. Flame* 172 (2016), pp. 349–364.

[21] K A Heufer and H Olivier. "Determination of ignition delay times of different hydrocarbons in a new high pressure shock tube". In: *Shock Waves* 20.4 (2010), pp. 307–316.

[22] Chenglong Tang, Liangjie Wei, Jiaxiang Zhang, Xingjia Man, and Zuohua Huang. "Shock Tube Measurements and Kinetic Investigation on the Ignition Delay Times of Methane/Dimethyl Ether Mixtures". In: *Energy Fuels* 26.11 (2012), pp. 6720–6728.

[23] Yingjia Zhang, Xue Jiang, Liangjie Wei, Jiaxiang Zhang, Chenglong Tang, and Zuohua Huang. "Experimental and modeling study on auto-ignition characteristics of methane/hydrogen blends under engine relevant pressure". In: *Int. J. Hydrog. Energy* 37.24 (2012), pp. 19168–19176.

[24] Yingjia Zhang, Zuohua Huang, Liangjie Wei, Jiaxiang Zhang, and Chung K Law. "Experimental and modeling study on ignition delays of lean mixtures of methane, hydrogen, oxygen, and argon at elevated pressures". In: *Combust. Flame* 159.3 (2012), pp. 918–931.

[25] Christopher J Aul, Wayne K Metcalfe, Sinéad M Burke, Henry J Curran, and Eric L Petersen. "Ignition and kinetic modeling of methane and ethane fuel blends with oxygen: A design of experiments approach". In: *Combust. Flame* 160.7 (2013), pp. 1153–1167.

[26] Alexander Burcat, Karl Scheller, and Assa Lifshitz. "Shock-tube investigation of comparative ignition delay times for C_1–C_5 alkanes". In: *Combust. Flame* 16.1 (1971), pp. 29–33.

[27] Assa Lifshitz, Karl Scheller, Alexander Burcat, and Gordon B Skinner. "Shock-tube investigation of ignition in methane-oxygen-argon mixtures". In: *Combust. Flame* 16.3 (1971), pp. 311–321.

[28] E K Dabora. "Effect of NO_2 on the ignition delay of CH_4-air mixtures". In: *Combust. Flame* 24.0 (1975), pp. 181–184.

[29] L J Spadaccini and M B Colket. "Ignition delay characteristics of methane fuels". In: *Prog. Energy Combust. Sci.* 20.5 (1994), pp. 431–460.

[30] Eric L Petersen, Michael Röhrig, David F Davidson, Ronald K Hanson, and Craig T Bowman. "High-pressure methane oxidation behind reflected shock waves". In: *Symp. (Int.) Combust., [Proc.]* 26.1 (1996), pp. 799–806.

[31] E L Petersen, D F Davidson, and R K Hanson. "Kinetics modeling of shock-induced ignition in low-dilution CH_4/O_2 mixtures at high pressures and intermediate temperatures". In: *Combust. Flame* 117.1-2 (1999), pp. 272–290.

[32] Eric L Petersen, David F Davidson, and Ronald K Hanson. "Ignition delay times of Ram accelerator CH_4/O_2/diluent mixtures". In: *J. Propul. Power* 15.1 (1999), pp. 82–91.

[33] X J Gu, M Z Haq, M Lawes, and R Woolley. "Laminar burning velocity and Markstein lengths of methane/air mixtures". In: *Combust. Flame* 121.1-2 (2000), pp. 41–58.

[34] Patricia Dirrenberger, Hervé Le Gall, Roda Bounaceur, Olivier Herbinet, Pierre-Alexandre Glaude, Alexander Konnov, and Frédérique Battin-Leclerc. "Measurements of laminar flame velocity for components of natural gas". In: *Energy Fuels* 25.9 (2011), pp. 3875–3884.

[35] G Rozenchan, D L Zhu, C K Law, and S D Tse. "Outward propagation, burning velocities, and chemical effects of methane flames up to 60 atm". In: *Proc. Combust. Inst.* 29.2 (2002), pp. 1461–1470.

[36] Emilien Varea, Vincent Modica, Alexis Vandel, and Bruno Renou. "Measurement of laminar burning velocity and Markstein length relative to fresh gases using a new postprocessing procedure: Application to laminar spherical flames for methane, ethanol and isooctane/air mixtures". In: *Combust. Flame* 159.2 (2012), pp. 577–590.

[37] Mayuri Goswami, Sander C R Derks, Kris Coumans, Willemyn J Slikker, Marcelo H de Andrade Oliveira, Rob J M Bastiaans, Carlo C M Luijten, L Philipus H de Goey, and Alexander A Konnov. "The effect of elevated pressures on the laminar burning velocity of methane + air mixtures". In: *Combust. Flame* 160.9 (2013), pp. 1627–1635.

[38] Toni Tahtouh, Fabien Halter, and Christine Mounaim-Rousselle. "Measurement of laminar burning speeds and Markstein lengths using a novel methodology". In: *Combust. Flame* 156.9 (2009), pp. 1735–1743.

[39] William Lowry, Jaap de Vries, Michael Krejci, Eric Petersen, Zeynep Serinyel, Wayne Metcalfe, Henry Curran, and Gilles Bourque. "Laminar Flame Speed Measurements and Modeling of Pure Alkanes and Alkane Blends at Elevated Pressures". In: *J. Eng. Gas Turbines Power* 133.9 (2011), p. 91501.

[40] Hamid Hashemi, Jon G Jacobsen, Christian T Rasmussen, Jakob M Christensen, Peter Glarborg, Sander Gersen, Martijn van Essen, Howard B Levinsky, and Stephen J Klippenstein. "High-pressure oxidation of ethane". In: *Combust. Flame* 182 (2017), pp. 150–166.

[41] Jiaxiang Zhang, Erjiang Hu, Lun Pan, Zihang Zhang, and Zuohua Huang. "Shock-Tube Measurements of Ignition Delay Times for the Ethane/Dimethyl Ether Blends". In: *Energy Fuels* 27.10 (2013), pp. 6247–6254.

[42] Lun Pan, Yingjia Zhang, Jiaxiang Zhang, Zemin Tian, and Zuohua Huang. "Shock tube and kinetic study of $C_2H_6/H_2/O_2/Ar$ mixtures at elevated pressures". In: *Int. J. Hydrog. Energy* 39.11 (2014), pp. 6024–6033.

[43] Erjiang Hu, Yizhen Chen, Zihang Zhang, Xiaotian Li, Yu Cheng, and Zuohua Huang. "Experimental study on ethane ignition delay times and evaluation of chemical kinetic models". In: *Energy Fuels* 29.7 (2015), pp. 4557–4566.

[44] Christine M Vagelopoulos and Fokion N Egolfopoulos. "Direct experimental determination of laminar flame speeds". In: *Symp. (Int.) Combust., [Proc.]* 27.1 (1998), pp. 513–519.

[45] Alexander A Konnov, Igor V Dyakov, and Jacques De Ruyck. "Measurement of adiabatic burning velocity in ethane-oxygen-nitrogen and in ethane-oxygen-argon mixtures". In: *Exp. Therm. Fluid Sci.* 27.4 (2003), pp. 379–384.

[46] G Jomaas, X L Zheng, D L Zhu, and C K Law. "Experimental determination of counterflow ignition temperatures and laminar flame speeds of C_2-C_3 hydrocarbons at atmospheric and elevated pressures". In: *Proc. Combust. Inst.* 30.1 (2005), pp. 193–200.

[47] Igor V Dyakov, Jacques De Ruyck, and Alexander A Konnov. "Probe sampling measurements and modeling of nitric oxide formation in ethane+air flames". In: *Fuel* 86.1-2 (2007), pp. 98–105.

[48] Mayuri Goswami. "Laminar burning velocities at elevated pressures using the heat flux method". PhD thesis. Technische Universiteit Eindhoven, 2014.

[49] S Ravi, T G Sikes, A Morones, C L Keesee, and E L Petersen. "Comparative study on the laminar flame speed enhancement of methane with ethane and ethylene addition". In: *Proc. Combust. Inst.* 35.1 (2015), pp. 679–686.

[50] M Cathonnet, J C Boettner, and H James. "Experimental study and numerical modeling of high temperature oxidation of propane and n-butane". In: *Symp. Combust.* 18.1 (1981), pp. 903–913.

[51] D N Koert, D L Miller, and N P Cernansky. "Experimental studies of propane oxidation through the negative temperature coefficient region at 10 and 15 atmospheres". In: *Combust. Flame* 96.1–2 (1994), pp. 34–49.

[52] Philip Cadman, Geraint O Thomas, and Philip Butler. "The auto-ignition of propane at intermediate temperatures and high pressures". In: *Phys. Chem. Chem. Phys.* 2.23 (2000), pp. 5411–5419.

[53] Jürgen Herzler, Ludger Jerig, and Paul Roth. "Shock-tube study of the ignition of propane at intermediate temperatures and high pressures". In: *Combust. Sci. Technol.* 176.10 (2004), pp. 1627–1637.

[54] F Norman, F Van den Schoor, and F Verplaetsen. "Auto-ignition and upper explosion limit of rich propane–air mixtures at elevated pressures". In: *J. Hazard. Mater.* 137.2 (2006), pp. 666–671.

[55] S M Gallagher, H J Curran, W K Metcalfe, D Healy, J M Simmie, and G Bourque. "A rapid compression machine study of the oxidation of propane in the negative temperature coefficient regime". In: *Combust. Flame* 153.1–2 (2008), pp. 316–333.

[56] Kai J Morganti, Michael J Brear, Gabriel da Silva, Yi Yang, and Frederick L Dryer. "The autoignition of Liquefied Petroleum Gas (LPG) in spark-ignition engines". In: *Proc. Combust. Inst.* 35.3 (2015), pp. 2933–2940.

[57] P Sabia, M de Joannon, G Sorrentino, P Giudicianni, and R Ragucci. "Effects of mixture composition, dilution level and pressure on auto-ignition delay times of propane mixtures". In: *Chem. Eng. J.* 277 (2015), pp. 324–333.

[58] H Hashemi, J M Christensen, and P Glarborg. "High-pressure oxidation of propane". To be submitted. 2018.

[59] H Hashemi, J M Christensen, and P Glarborg. "High-pressure oxidation of butane". To be submitted. 2018.

[60] D Healy, N S Donato, C J Aul, E L Petersen, C M Zinner, G Bourque, and H J Curran. "n-Butane: Ignition delay measurements at high pressure and detailed chemical kinetic simulations". In: *Combust. Flame* 157.8 (2010), pp. 1526–1539.

[61] Nicole Donato, Christopher Aul, Eric Petersen, Christopher Zinner, Henry Curran, and Gilles Bourque. "Ignition and oxidation of 50/50 butane isomer blends". In: *J. Eng. Gas Turbines Power* 132.5 (2010), p. 051502.

[62] S Gersen, AV Mokhov, JH Darmeveil, and HB Levinsky. "Ignition properties of n-butane and iso-butane in a rapid compression machine". In: *Combust. Flame* 157.2 (2010), pp. 240–245.

[63] Christian Lund Rasmussen, Karin Hedebo Wassard, Kim Dam-Johansen, and Peter Glarborg. "Methanol oxidation in a flow reactor: Implications for the branching ratio of the CH_3OH+OH reaction". In: *Int. J. Chem. Kinet.* 40.7 (2008), pp. 423–441.

[64] Hamid Hashemi, Jakob M Christensen, Sander Gersen, and Peter Glarborg. "Hydrogen oxidation at high pressure and intermediate temperatures: Experiments and kinetic modeling". In: *Proc. Combust. Inst.* 35.1 (2015), pp. 553–560.

[65] H Hashemi, J M Christensen, and P Glarborg. "Ethanol oxidation at high pressure". Submitted. 2017.

[66] *Deliverable: D2.4, Modeling of multi-fuel ignition (part A)*. Tech. rep. `http://www.hercules-2.com/`. HERCULES-2 project, 2017.

[67]   *Deliverable: D2.5, Characterization of multi-fuel ignition and combustion.* Tech. rep. `http://www.hercules-2.com/`. HERCULES-2 project, 2018.

[68]   J. Hult and C. Kunkel. "*HERCULESII, WP2: Multi-fuel combustion*". In: PTB meeting (Zurich). 2017.

[69]   Federico Piscaglia. "Faster and Open engine Simulations for automotive Industry". In: *Place Digest* 2 (2013), 13–14.

[70]   A. Montorfano, F. Piscaglia, and A Onorati. "An Extension of the Dynamic Mesh Handling with Topological Changes for LES of ICE in OpenFOAM". In: (2015). `http://dx.doi.org/10.4271/2015-01-0384`.

[71]   F. Piscaglia, A. Montorfano, and A. Onorati. "A Moving Mesh Strategy to Perform Adaptive Large Eddy Simulation of IC Engines in OpenFOAM". In: *International Multidimensional Engine Modeling User's Group Meeting 2014, The Detroit Downtown Courtyard by Marriott Hotel, Detroit, MI (USA)*. `https://imem.cray.com/2014/Meeting-2014/9-Piscaglia-Milano-IMEM2014.pdf`. 2014.

[72]   F. Piscaglia, A. Montorfano, and A. Onorati. "A Compressible Dynamic Solver for the Simulation of Turbulent Flows in IC Engine Geometries". In: *International Multidimensional Engine Modeling User's Group Meeting At the SAE Congress*. `https://imem.cray.com/2015/Meeting-2015/12-IMEM2015-Milano.pdf`. 2015.

[73]   F. Piscaglia, A. Montorfano, et al. "Hybrid RANS/LES of Moving Boundary Problems: Application to Cavitating Sprays and In-Cylinder Flows". In: *International Multidimensional Engine Modeling User's Group Meeting At the SAE Congress*. `https://imem.cray.com/agenda.html`. 2016.

[74]   F. Piscaglia. "*Developments in Transient Modeling, Moving Mesh, Turbulence and Multiphase Methodologies in OpenFOAM*". In: Keynote Lecture at The 4th Annual OpenFOAM User Conference 2016 [link]. 2016.

[75]   M. Jangi, R. Yu, and X. S. Bai. "A multi-zone chemistry mapping approach for direct numerical simulation of auto-ignition and flame propagation in a constant volume enclosure". In: *Combustion Theory and Modelling* 16.2 (2012), pp. 221–249. eprint: `http://dx.doi.org/10.1080/13647830.2011.608858`.

[76]   G. D'Errico, T. Lucchini, F. Contino, M. Jangi, and X.-S. Bai. "Comparison of well-mixed and multiple representative interactive flamelet approaches for diesel spray combustion modelling". In: *Combustion Theory and Modelling* 18.1 (2014), pp. 65–88.

[77]   Tong Yao, Yuanjiang Pei, Bei-Jing Zhong, Sibendu Som, Tianfeng Lu, and Kai Hong Luo. "A compact skeletal mechanism for n-dodecane with optimized semi-global low-temperature chemistry for diesel engine simulations". In: *Fuel* 191 (2017), pp. 339 –349.

[78]   R S Tranter, H Ram Amoorthy, A Raman, K Brezinsky, and M D Allendorf. "High-pressure single-pulse shock tube investigation of rich and stoichiometric ethane oxidation". In: *Proc. Combust. Inst.* 29.1 (2002), pp. 1267–1275.

[79]   R S Tranter, R Sivaramakrishnan, K Brezinsky, and M D Allendorf. "High pressure, high temperature shock tube studies of ethane pyrolysis and oxidation". In: *Phys. Chem. Chem. Phys.* 4.11 (2002), pp. 2001–2010.

[80] F N Egolfopoulos, D L Zhu, and C K Law. "Experimental and numerical determination of laminar flame speeds: Mixtures of C2-hydrocarbons with oxygen and nitrogen". In: *Symp. (Int.) Combust., [Proc.]* 23.1 (1991), pp. 471–478.

[81] M I Hassan, K T Aung, O C Kwon, and G M Faeth. "Properties of laminar premixed hydrocarbon/air flames at various pressures". In: *J. Propul. Power* 14.4 (1998), pp. 479–488.

[82] Kamal Kumar, Gaurav Mittal, Chih-Jen Sung, and Chung K Law. "An experimental investigation of ethylene/O_2/diluent mixtures: Laminar flame speeds with preheat and ignition delays at high pressures". In: *Combust. Flame* 153.3 (2008), pp. 343–354.

[83] Emad Rokni, Ali Moghaddas, Omid Askari, and Hameed Metghalchi. "Measurement of laminar burning speeds and investigation of flame stability of acetylene C_2H_2/air mixtures". In: *J. Energy Resour. Technol.* 137.1 (2015), p. 012204.

[84] L R Cancino, M Fikri, A A M Oliveira, and C Schulz. "Measurement and Chemical Kinetics Modeling of Shock-Induced Ignition of Ethanol-Air Mixtures". In: *Energy Fuels* 24.5 (2010), pp. 2830–2840.

[85] K E Noorani, B Akih-Kumgeh, and J M Bergthorson. "Comparative high temperature shock tube ignition of C_1–C_4 primary alcohols". In: *Energy Fuels* 24.11 (2010), pp. 5834–5843.

[86] Changyoul Lee, Stijn Vranckx, Karl A Heufer, Sergey V Khomik, Yasar Uygun, Herbert Olivier, and Ravi X Fernandez. "On the Chemical Kinetics of Ethanol Oxidation: Shock Tube, Rapid Compression Machine and Detailed Modeling Study". In: *Z. Phys. Chem.* 226.1 (2012), pp. 1–28.

[87] Gaurav Mittal, Sinead M Burke, Varun A Davies, Bikash Parajuli, Wayne K Metcalfe, and Henry J Curran. "Autoignition of ethanol in a rapid compression machine". In: *Combust. Flame* 161.5 (2014), pp. 1164–1171.

[88] Cesar L Barraza-Botet, Scott W Wagnon, and Margaret S Wooldridge. "Combustion Chemistry of Ethanol: Ignition and Speciation Studies in a Rapid Compression Facility". In: *J. Phys. Chem. A* 120.38 (2016), pp. 7408–7418.

[89] Frederick L Dryer and Marcos Chaos. "Ignition of syngas/air and hydrogen/air mixtures at low temperatures and high pressures: Experimental data interpretation and kinetic modeling implications". In: *Combust. Flame* 152.1–2 (2008), pp. 293–299.

[90] Marcos Chaos and Frederick L Dryer. "Chemical-kinetic modeling of ignition delay: Considerations in interpreting shock tube data". In: *Int. J. Chem. Kinet.* 42.3 (2010), pp. 143–150.

[91] Omer L Gulder. "Laminar burning velocities of methanol, ethanol and isooctane-air mixtures". In: *Symp. (Int.) Combust., [Proc.]* 19.1 (1982), pp. 275–281.

[92] F N Egolfopoulos, D X Du, and C K Law. "A study on ethanol oxidation kinetics in laminar premixed flames, flow reactors, and shock tubes". In: *Symp. Combust.* 24.1 (1992), pp. 833–841.

[93] D Bradley, M Lawes, and M S Mansour. "Explosion bomb measurements of ethanol-air laminar gaseous flame characteristics at pressures up to 1.4 MPa". In: *Combust. Flame* 156.7 (2009), pp. 1462–1470.

[94] AA Konnov, RJ Meuwissen, and LPH De Goey. "The temperature dependence of the laminar burning velocity of ethanol flames". In: *Proc. Combust. Inst.* 33.1 (2011), pp. 1011–1019.

[95] J P J van Lipzig, E J K Nilsson, L P H de Goey, and A A Konnov. "Laminar burning velocities of n-heptane, iso-octane, ethanol and their binary and tertiary mixtures". In: *Fuel* 90.8 (2011), pp. 2773–2781.

[96] Kian Eisazadeh-Far, Ali Moghaddas, Jalal Al-Mulki, and Hameed Metghalchi. "Laminar burning speeds of ethanol/air/diluent mixtures". In: *Proc. Combust. Inst.* 33.1 (2011), pp. 1021–1027.

[97] Louis Sileghem, VA Alekseev, Jeroen Vancoillie, EJK Nilsson, Sebastian Verhelst, and AA Konnov. "Laminar burning velocities of primary reference fuels and simple alcohols". In: *Fuel* 115 (2014), pp. 32–40.

[98] Patricia Dirrenberger, Pierre-Alexandre Glaude, Roda Bounaceur, Hervé Le Gall, A Pires da Cruz, AA Konnov, and F Battin-Leclerc. "Laminar burning velocity of gasolines with addition of ethanol". In: *Fuel* 115 (2014), pp. 162–169.

Appendices

A   Methane: further validation

Further evaluation against flow-reactor data: methane

The model is further evaluated against data from experiments in the DTU flow-reactor for fuel-rich and fuel-lean conditions. Figure 39 presents the gas composition at the reactor outlet under reducing conditions (Φ=19.7) for different isotherms. The consumption of reactants starts at 725 K, and the major product of the partial oxidation of methane is CO at all investigated temperatures. Upon ignition, considerable amounts of formaldehyde and methanol are formed but their fractions gradually decline at higher temperatures. Above 750 K, C_2H_6 and C_2H_4 are formed to greater extents. At 900 K, the major products are CO and C_2H_6. The model predicts the onset of reaction as well as the concentrations of CH_4, O_2, CO, and C_2H_6 very well. However, CO_2 and in particular CH_3OH are underpredicted while CH_2O is overpredicted. The discrepancies for these species cannot be explained by the experimental uncertainties (shown as error bars in the figure). The observed levels of CH_3OH are in agreement with the measurements under similar conditions by Rasmussen et al. [7].

The methane oxidation under very oxidizing conditions (Φ=0.06) starts at 750 K. The major products are CO and CO_2 (Fig. 40). The CO concentration peaks at 775 K but declines gradually at higher temperatures where CO is oxidized to CO_2. The model predicts well the onset of reaction and the methane consumption upon ignition, but above 775 K CO is slightly overpredicted while again CO_2 is underestimated.
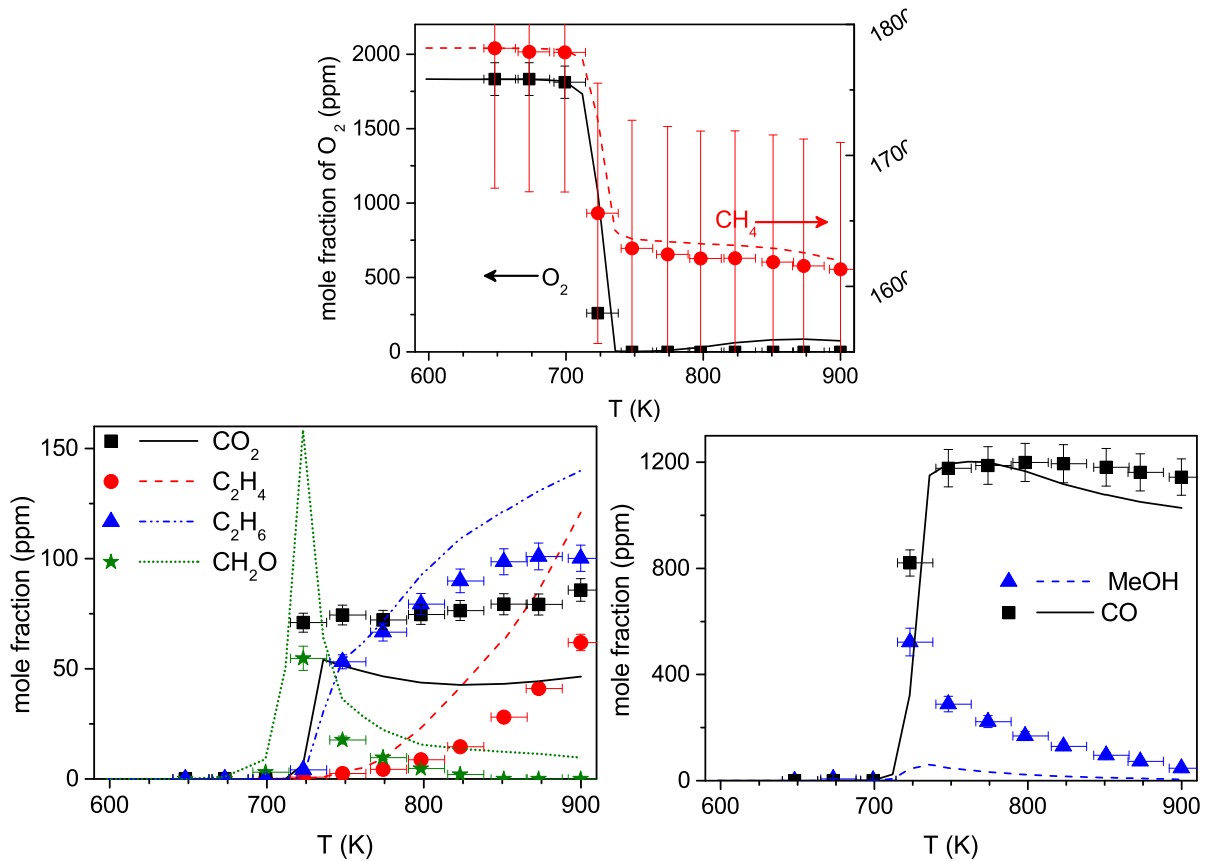
Figure 39: Results of experiments under reducing conditions (0.18% O_2 and 1.75% CH_4 in N_2, Φ=19.7) at 100 bar pressure. Symbols mark the experimental results and lines denote the predictions of the present model. The temperature profile was implemented in the simulations. Considering only the isothermal zone of the reactor (± 6 K, residence time=9586/T [s]) deteriorates slightly the agreement.
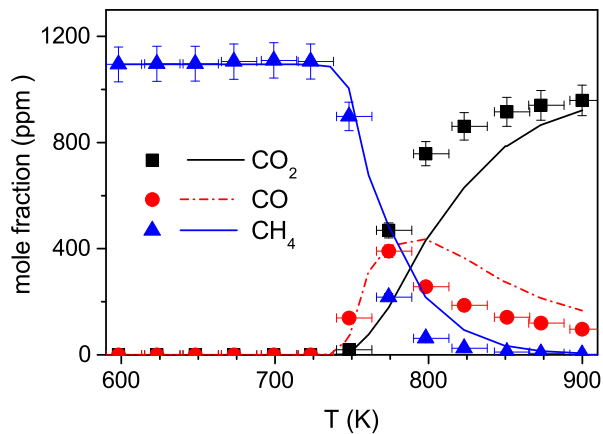

Figure 40: Results of experiments under oxidizing conditions (3.96% O_2 and 0.11% CH_4 in N_2, Φ=0.06) at 100 bar pressure. Symbols mark the experimental results and lines denote the predictions of the present model. The temperature profile was implemented in the simulations. Considering only the isothermal zone of the reactor (± 6 K, residence time=9586/T [s]) deteriorates slightly the agreement.

Further evaluation against ignition delays: methane

The oxidation of methane has been investigated extensively in shock tubes [1, 2, 12, 14, 21–32]. Davidson and Hanson [14] measured the ignition delays of methane at pressures up to 156 atm and temperatures of 1137–1536 K. A selection of their results is shown in Fig. 41. As expected, the ignition delay decreases with increasing pressure or temperature, being most sensitive to temperature. The ignition is faster for fuel-lean mixtures although those mixtures had a slightly higher dilution (77% Ar) compared to the fuel-rich mixtures (67% Ar). The predictions compare well with the experimental results, especially at higher pressures. The model is also accurate in simulating the results by Petersen et al. [32] who measured the ignition delays at pressures up to 261 atm (see Fig. 42).
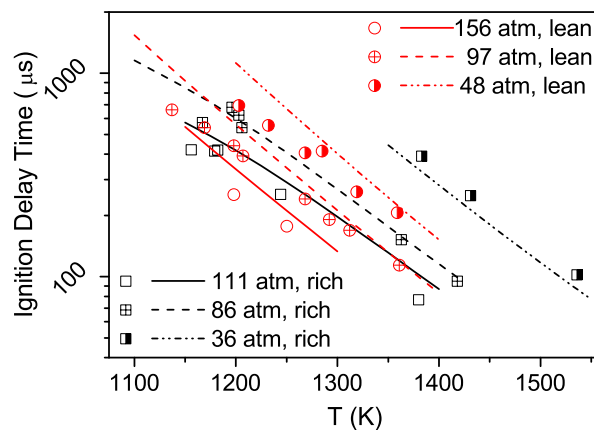
Figure 41: Ignition delay times of fuel-lean (3.8% CH_4+19.2% O_2 in Ar, Φ=0.4) and fuel-rich (20.0% CH_4+13.3% O_2 in Ar, Φ=3) mixtures. Symbols mark experimental results from Davidson and Hanson [14] and lines denotes the predictions of the present model. The simulations are conducted at fixed pressures while the pressure in the experiments fluctuated within ±10%.

Figure 42: Ignition delay times of fuel-rich (Φ=3) mixtures of CH_4/O_2 in inert gases (55–67% of Ar or N_2) . Symbols mark experimental results from Petersen et al. [32] and lines denotes the predictions of the present model. The simulations are conducted at fixed pressures while the pressure in the experiments fluctuated within $\pm 10\%$.
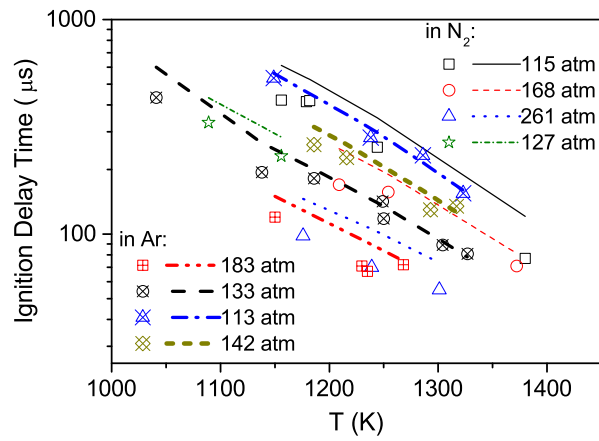
B   Ethane: further validation

Further evaluation against flow-reactor data: ethane

Figure 43 presents the results of experiments for fuel-rich mixtures (ϕ=37–47) at pressures of 20, 50, and 100 bar. At 20 bar pressure the fuel consumption starts at 775 K. Ethene and to a lesser extent CO and CH_4 are the major products. Increasing pressure to 50 and then 100 bar shifts the onset temperatures of the fuel conversion to 750 and 700 K, respectively.

The results under reducing conditions could indicate that ethane is oxidized in two stages. The fuel is consumed rapidly in the first stage, while as the temperature increases, the consumption of ethane becomes slow. This behavior, which is most pronounced at 100 bar, is caused by the depletion of O_2 and cannot be attributed to NTC type chemistry.

The model predictions for reducing conditions are in satisfactory agreement with measurements (Fig. 43). The model predicts the onset temperature of the fuel conversion accurately and trends are captured well. The major products, CO and CH_4, are slightly overpredicted while the sum of methanol and acetaldehyde is underpredicted. According to the model, acetaldehyde is formed to a greater extent than methanol, so the sum of them likely represents acetaldehyde formation.

For fuel-lean mixtures ($\phi = 0.034$–0.038) (Fig. 44), the fuel oxidation starts at temperatures close to those found for stoichiometric mixtures. Here, the major products are CO and CO_2. Similar to stoichiometric conditions, C_2H_4 peaks at intermediate temperatures and disappears at higher temperatures.

Further evaluation against shock-tube data: ethane

Tranter and coworkers have measured the concentration of stable components behind the shock in a shock tube at high pressures of 40 [78], as well as 340 and 613 bar [79]. The post-shock composition was measured by a GC. By recording pressure and calculating temperature accordingly, they were able to simulate the post-shock conditions.

To simulate the data, here a fixed pressure (40, 340, and 613 bar) and a residence time of 1.7 ms were implemented in the model. As shown in Fig. 45 for 40 bar, the
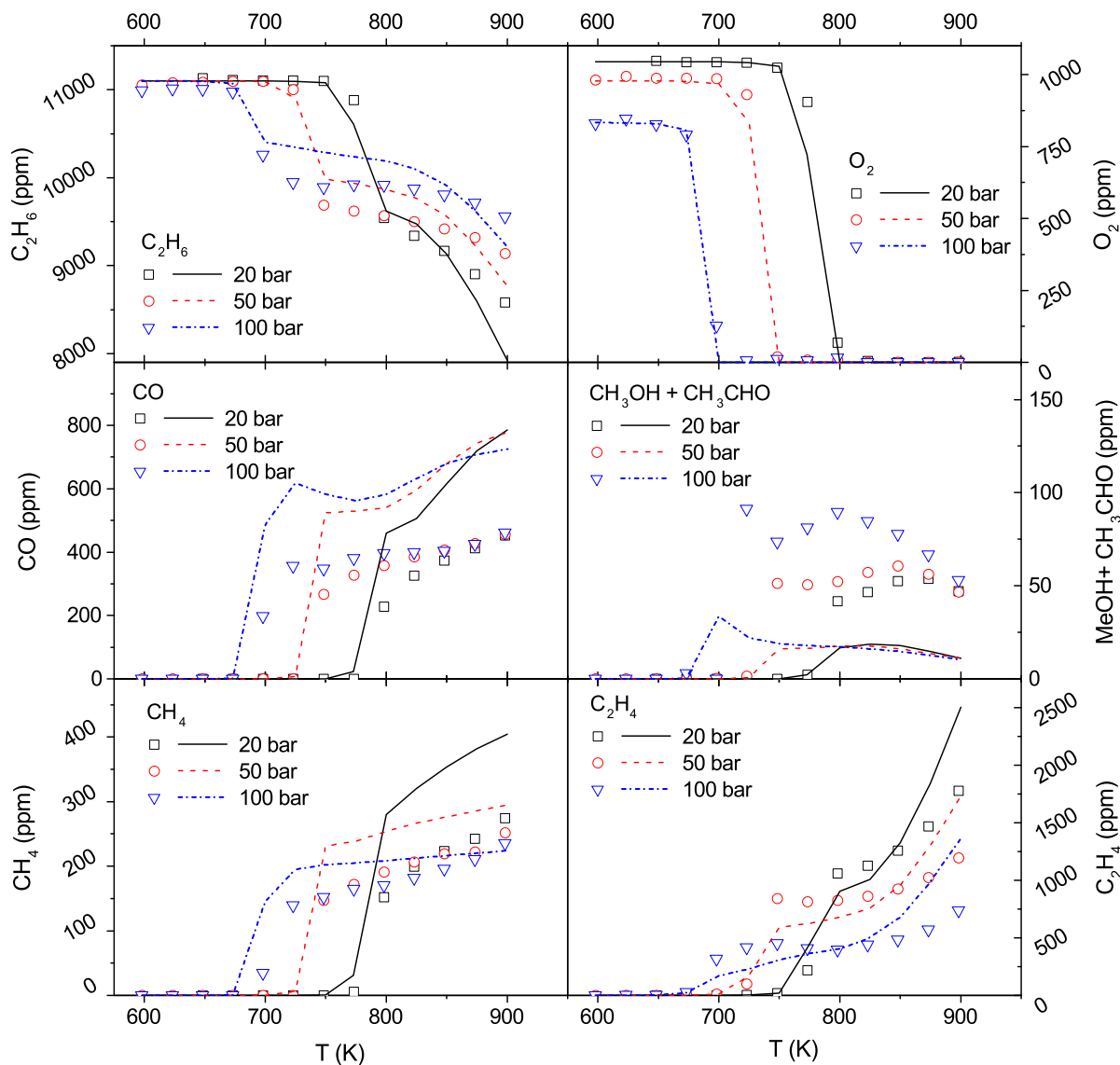
Figure 43: Results (molar fractions) of experiments under reducing conditions at 20 bar (ϕ=37.2, 11130/1044 ppm of C_2H_6/O_2), 50 bar (ϕ=39.7, 11055/978 ppm of C_2H_6/O_2), and 100 bar (ϕ=46.6, 10990/834 ppm of C_2H_6/O_2). All mixtures are diluted in nitrogen. Symbols mark experimental results and lines denote predictions of the present model using the temperature profiles in the supplementary materials. Approximating the gas residence time by τ=2525 / T [K] s (20 bar), τ=6204 / T [K] s (50 bar), and τ=12970/T [K] s (100 bar) may deteriorate the model predictions slightly.

fuel conversion starts around 1150 K and is accompanied by a gradual increase in the concentrations of CO and C_2H_4. Above 1250 K, the C_2H_4 concentration decreases and it almost disappears around 1400 K. At 340 and 613 bar, the fuel conversion is detected above 1075 K. The model generally agrees well with the measurements, even though at 340 bar the temperature for onset of oxidation is overpredicted by around 50 K.
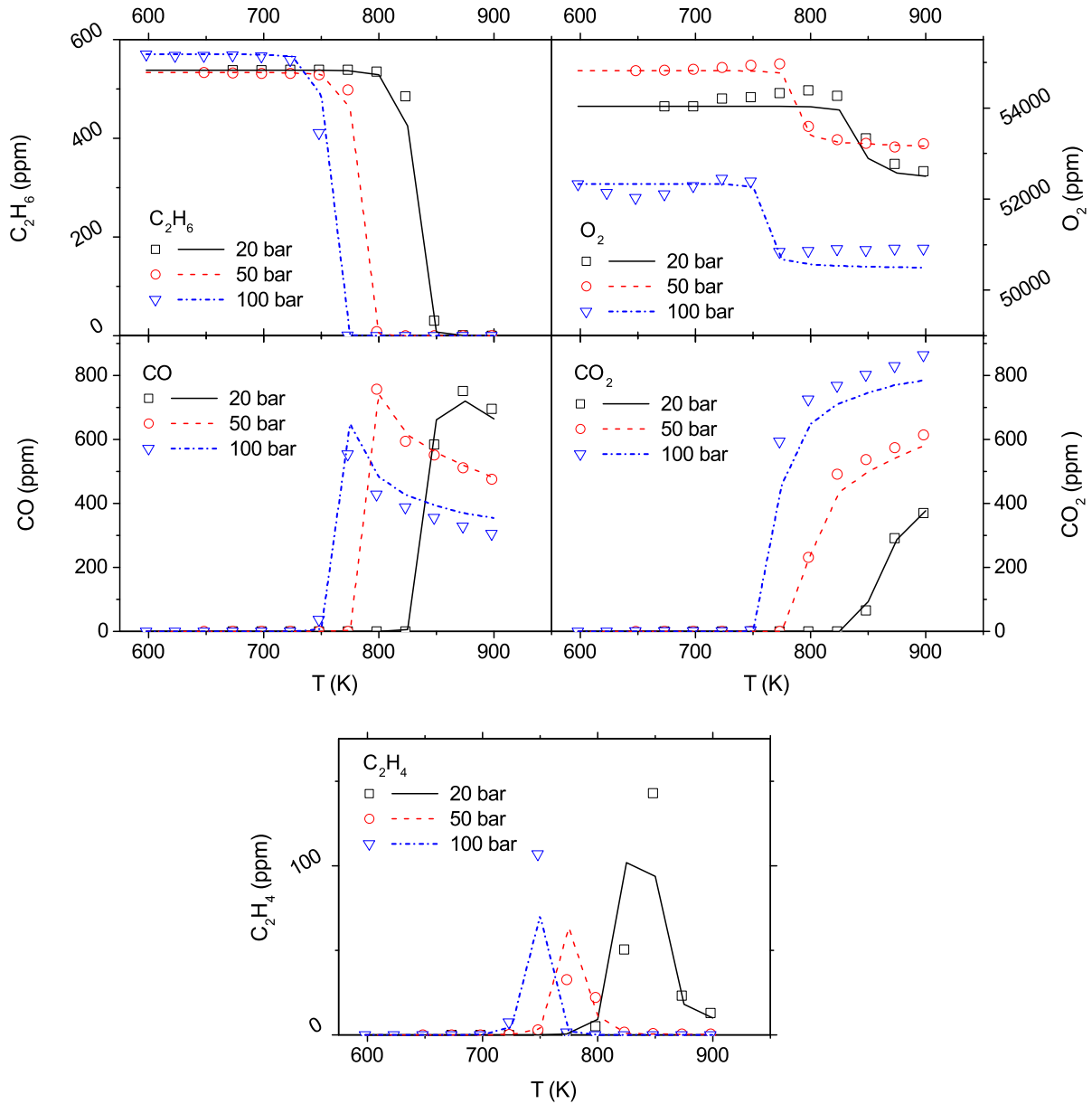
Figure 44: Results (molar fractions) of experiments under oxidizing conditions at 20 bar (ϕ=0.035, 538/54035 ppm of C_2H_6/O_2), 50 bar (ϕ=0.034, 533/54815 ppm of C_2H_6/O_2), and 100 bar (ϕ=0.038, 570/52335 ppm of C_2H_6/O_2). All mixtures are diluted in nitrogen. Symbols mark experimental results and lines denote predictions of the present model using the temperature profiles in the supplementary materials. Approximating the gas residence time by τ=2327/T [K] s (20 bar), τ=5950/T [K] s (50 bar), and τ=11890/T [K] s (100 bar) may deteriorate the model predictions slightly.

Further discussion of flame data: ethane

The reason for the overprediction of the ethane flame speed is not clear. The present model predicts the flame speeds of hydrogen, methane, and acetylene very well [19, 20,

64]. The calculated flame speeds of ethene and acetylene are shown in figure 46 for atmospheric pressure and the results are within the uncertainty range of the experimental measurements.
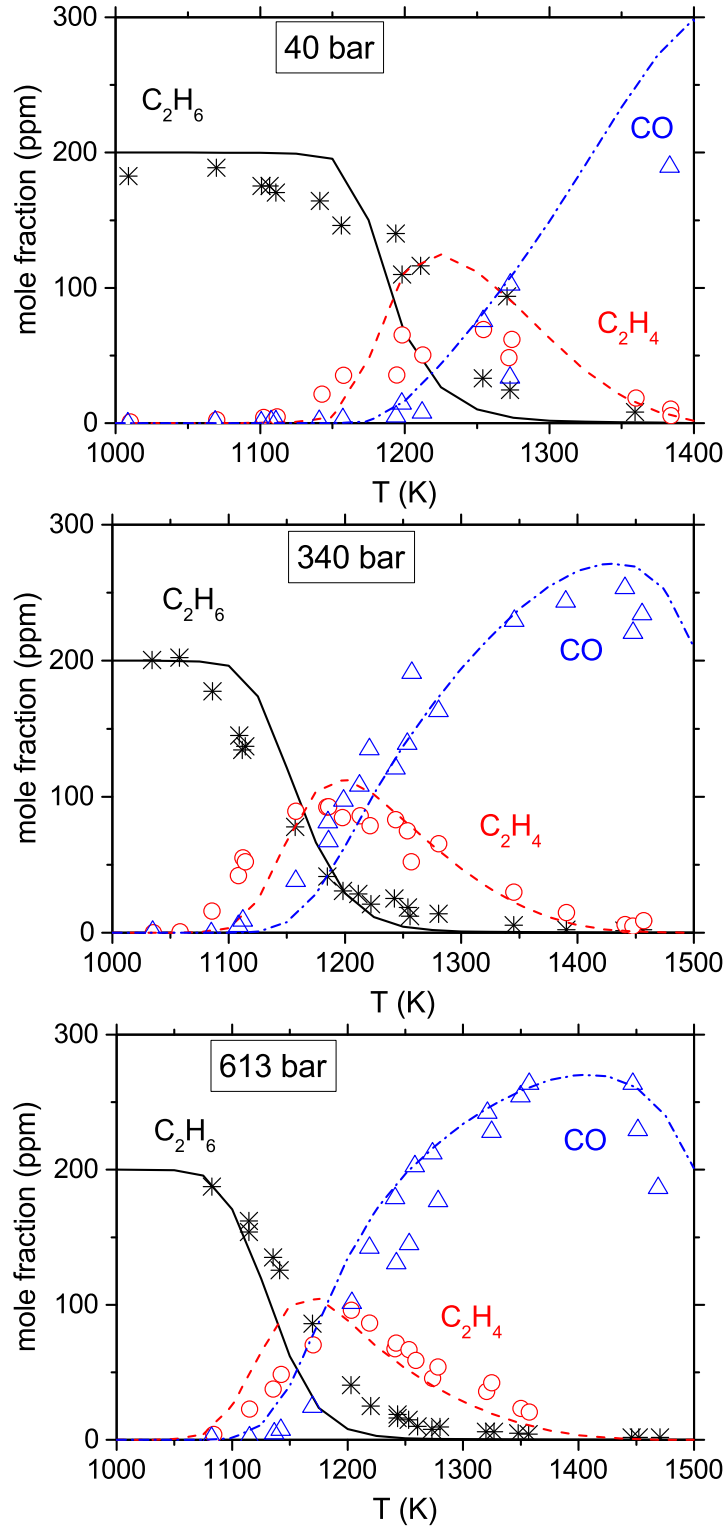
Figure 45: Post–shock concentration profiles at different temperatures. Symbols mark experimental results measured in a shock tube with initial mole fractions of 200 ppm of C_2H_6 ($\Phi=1$, in AR) at pressures of Top: 40 bar, from ref [78]; Middle: 340 bar, from ref [79]; Bottom: 613 bar, from ref [79]. Lines denote the prediction of the present model implementing a fixed residence time of 1.7 ms.
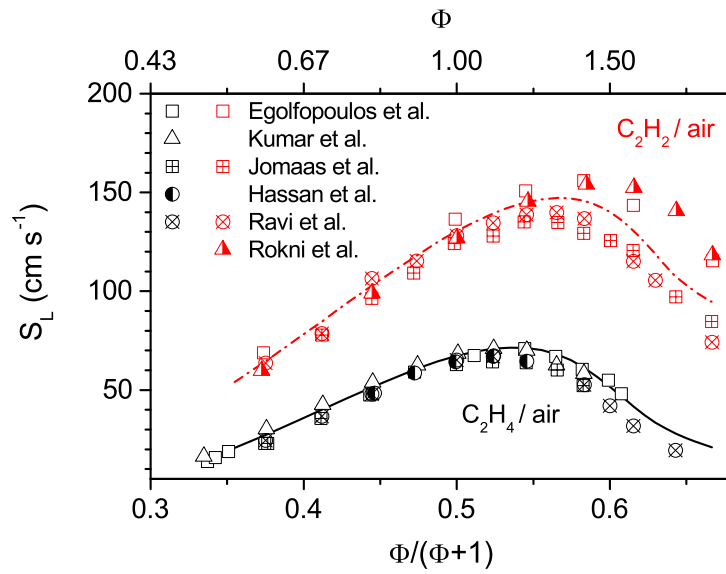
Figure 46: The unstretched laminar burning velocity of ethene/air and acetylene/air mixtures versus normalized equivalence ratio for an initial temperature of 300 K and at atmospheric pressure. Lines denote the present model predictions and symbols mark experimental results from Jomaas et al. [46], Ravi et al. [49], Egolfopoulos et al. [80], Hassan et al. [81], and Kumar et al. [82], and Rokni et al. [83].

C Propane: further validation

Further evaluation against flow-reactor data: propane

Figure 47 shows the results of propane oxidation for a fuel-rich mixture (reducing conditions). The fuel oxidation started at 700–725 K and the major detected products have been CO, C_3H_6, CH_4, and C_2H_4. The model was able to reproduce the onset of oxidation as well as the concentrations of intermediate components precisely.

The results of experiment for a fuel-lean mixture (oxidizing conditions) are shown in figure 48. At temperature above 600 K, propane concentration dropped sharply and propane vanished from the exhaust at T>725 K. The major detected products were CO and CO_2. The model predicted slower reactivity compared to the experiments, so the fuel conversion was slightly underpredicted by the model.
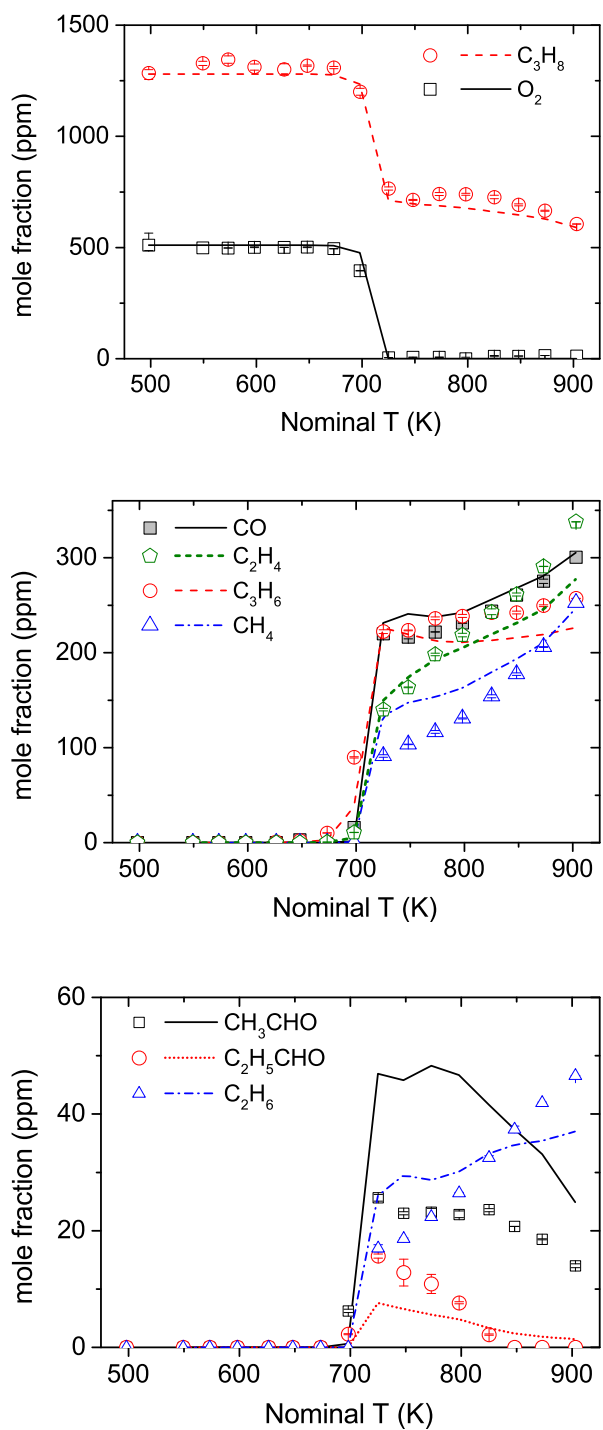
Figure 47: Results of experiments under reducing conditions (1285 ppm C_3H_8 and 511 ppm O_2 in N_2, $\Phi=12.5$) at 100 bar pressure. Symbols mark the experimental results and lines denote the predictions of the present model. The temperature profile was implemented in the simulations.
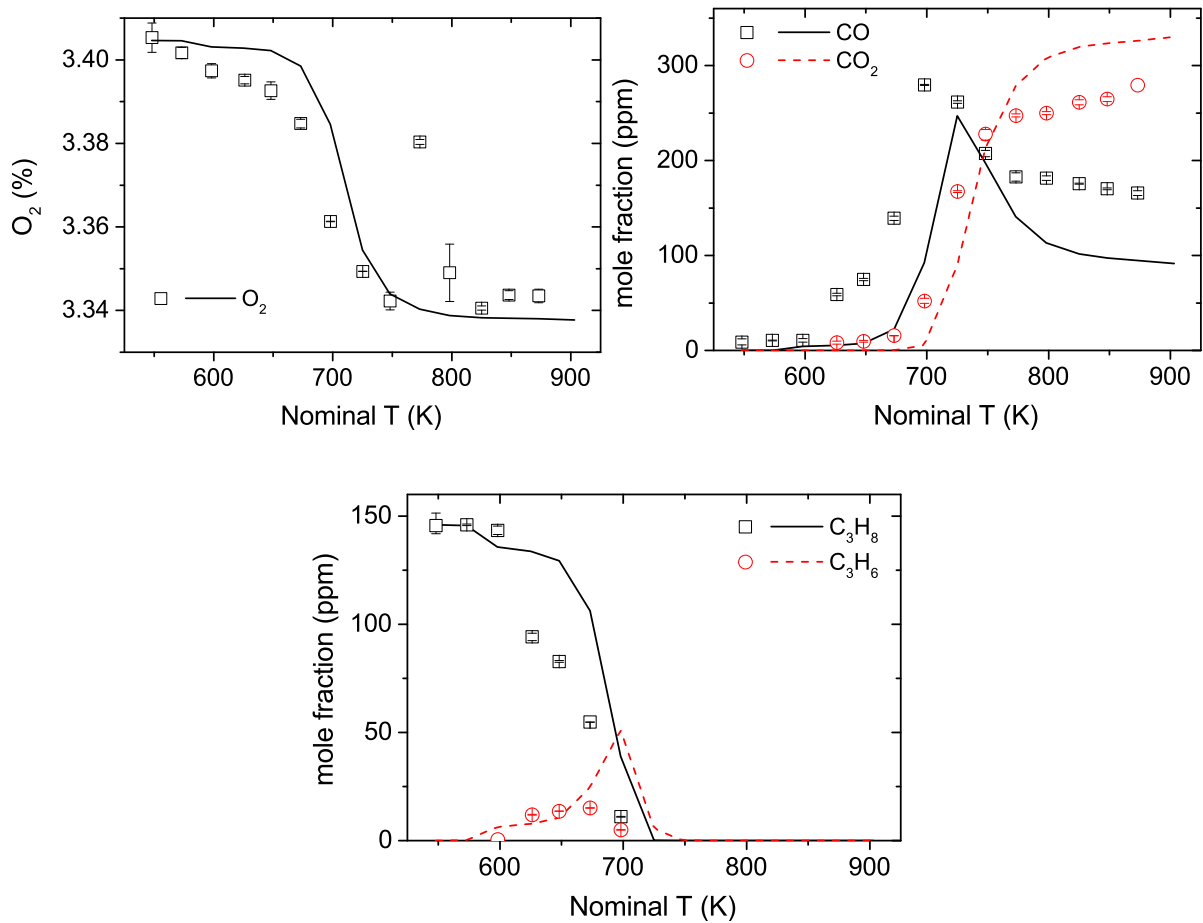
Figure 48: Results of experiments under oxidizing conditions (3.405% O_2 and 146 ppm C_3H_8 in N_2, Φ=0.02) at 100 bar pressure. Symbols mark the experimental results and lines denote the predictions of the present model. The temperature profile was implemented in the simulations.

D Ethanol: further validation

Further evaluation against flow-reactor data: ethanol

Figure 49 shows the results of the pyrolysis experiments. The ethanol conversion starts around 825 K and increases with temperature to 18% at 900 K. The major detected products are CH_4, CO, and C_2H_4. The present model predicts the onset temperature of ethanol decomposition well, but it slightly overestimates the chemical reactivity of ethanol at higher temperatures. The acetaldehyde yield from the model agrees well with the measurements at temperature below 875 K.

The ethanol conversion starts around 700 K for the fuel-rich mixture (Φ=43, see figure 50). Acetaldehyde and CO are the major detected products of ethanol partial oxidation. The model predicts well the onset temperature of reaction but it marginally underestimates the fuel conversion at high temperatures. Although the model overpredicts the concentrations of ethane and ethanol, it reproduces well the fractions of O_2, C_2H_4, and CH_3CHO.

For the fuel-lean mixture (Φ=0.10), the fuel oxidation is observed at temperatures above 725 K, similar to the onset temperature for stoichiometric and reducing mixtures. The model agrees well with to the measurements and the carbon is balanced by a maximum loss of 21% which occurs at 725 K.

Further evaluation against shock-tube data: ethanol

Figure 52 compares ethanol ignition delays calculated here with those reported in literature [21, 84–88]. The ignition delay decreases monotonically with increasing temperature and the model can predict the ignition delays fairly well for most of the cases above 900 K. However, it systematically overpredicts ignition delays measured in shock tube (top figure) at T<900 K. Meanwhile, the model agrees relatively better with measurements from RCM (bottom figure) at T<900 K.

The difference between RCM and shock tube data might be due to the pre-ignition pressure rise in shock tube experiments, as noted earlier [86, 87]. Over long residence times, pressure and temperature increase gradually behind the shock wave [86], even in

non-reactive mixtures [89, 90]. These pre-ignition effects are believed to be fuel-dependent and increase at lower temperatures [86]. In RCM, on the other hand, it is common to observe decreasing pressure (and temperature) due to heat transfer. In general, it is required to include those pre-ignition pressure variation in interpreting and simulating data for long residence time for both shock tubes and RCM. In the RCM data simulated here, the pre-ignition pressure-drop was reported to be fairly negligible and therefore is not included in the simulation. For the shock tube data from Cancino et al. [84], simulations are repeated by considering a pressure rise of 2% (per ms) behind the shock wave. The results (not shown here) improve but still deviate considerably from the measurements at T<900 K. We attribute the differences at least partly to device-dependent non-idealities in conducting experiments. More-controlled experiments in RCM and shock tubes might help to find the source of the data discrepancy at low temperature and high pressure.

Further evaluation against flame speed data: ethanol

Figure 53 compares the laminar burning velocity of ethanol/air mixtures calculated by the model with measured data [91–98]. At atmospheric pressure, the model slightly overpredicts the burning velocity but its prediction improves for fuel-rich mixtures. The trend of changes as well as the fuel-air equivalence ratio corresponding to the maximum flame speed are predicted well.

The model is further tested against data obtained at higher pressures of 5–12 bar by Gulder [91] and Bradley et al. [93]. To avoid ethanol condensation at high pressures, the initial temperature had to be increased. While the maximum flame speed at 5 and 7 bar occurred at $\Phi=1.1$ according to Gulder [91], it was reported at $\Phi=1.2$ by Bradley et al. [93]. This difference shifts the profiles and causes noticeable scattering between the data in the fuel-rich side. The model overestimates the flame speed at high pressures but its trend is similar to data from Gulder [91].
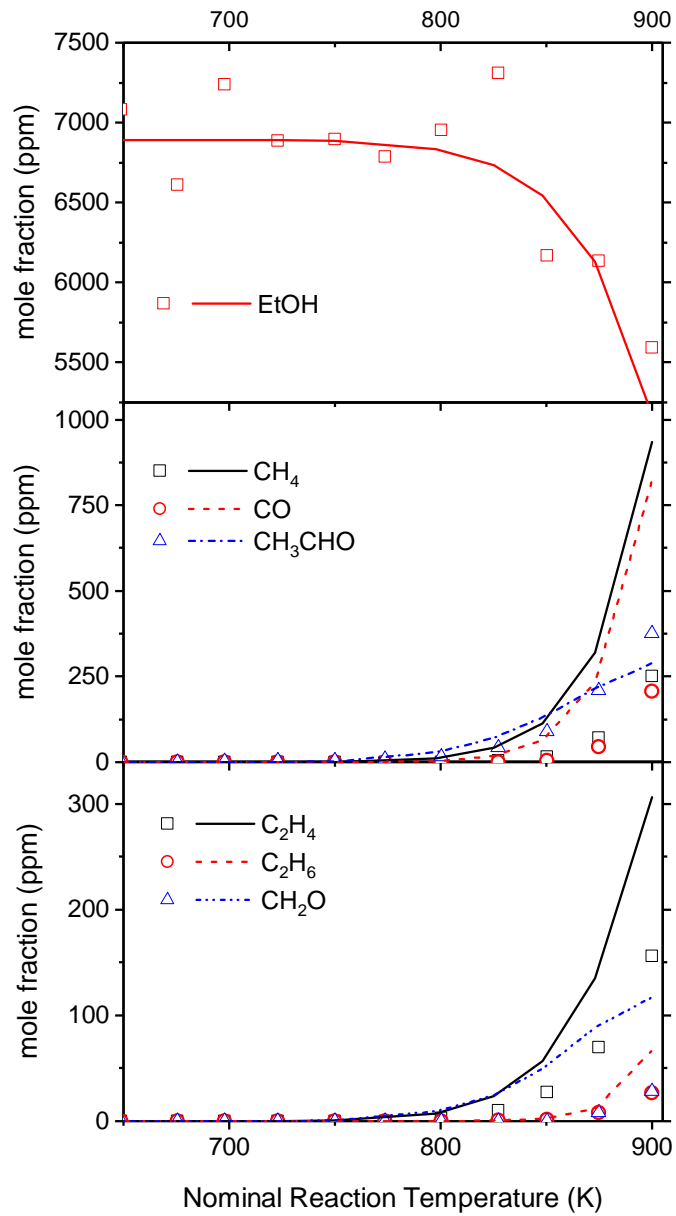
Figure 49: Results of pyrolysis experiments (0.689% ethanol in N_2) at 50 bar. Gas residence time is given by $\tau[s]=4098/T[K]$ ($\pm 8\%$).
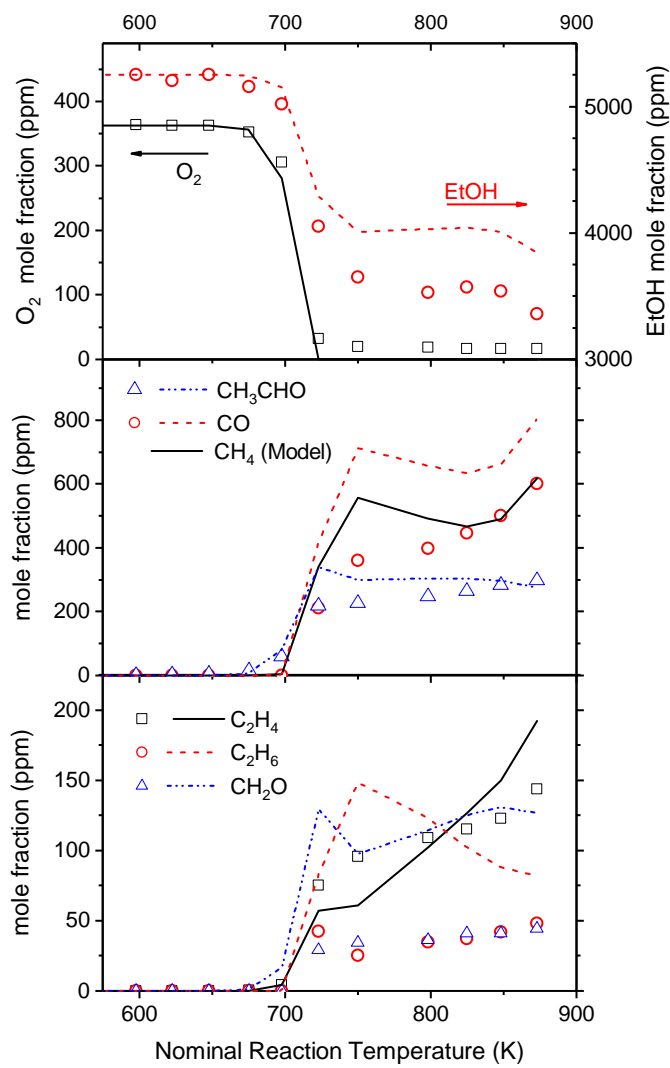
Figure 50: Results of experiments under reducing conditions (0.525% ethanol and 0.0363% O_2 in N_2, Φ=43) at 50 bar. Gas residence time is given by $\tau[s]$=3840/T[K] ($\pm$8%).

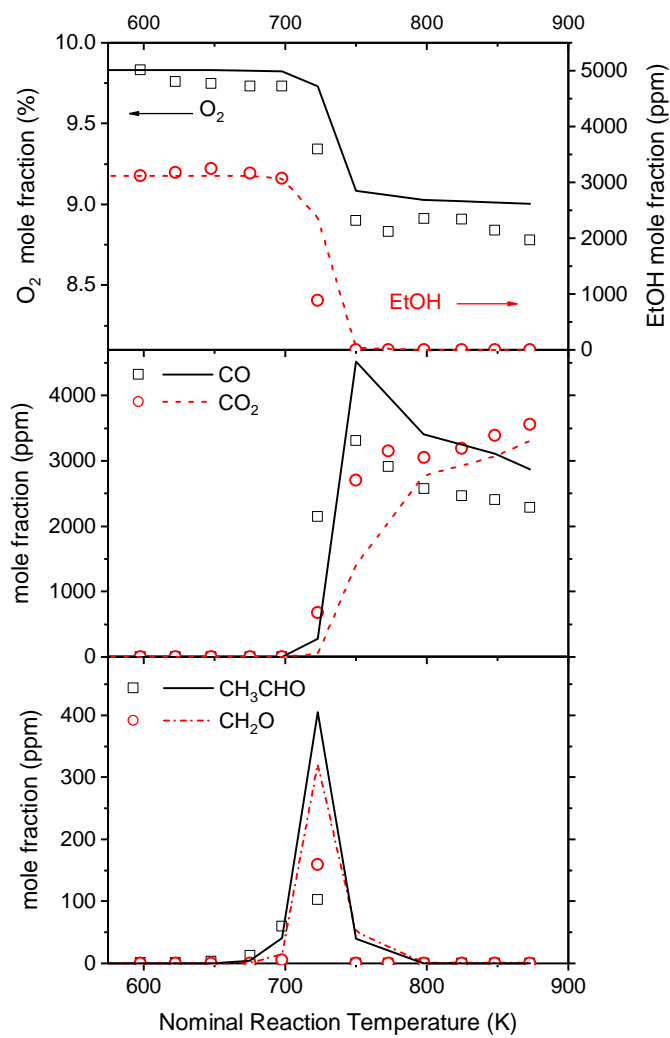Figure 51: Results of experiments under oxidizing conditions (0.312% ethanol and 9.830% O_2 in N_2, $\Phi=0.10$) at 50 bar. Gas residence time is given by $\tau[s]=3840/T[K]$ ($\pm 8\%$).
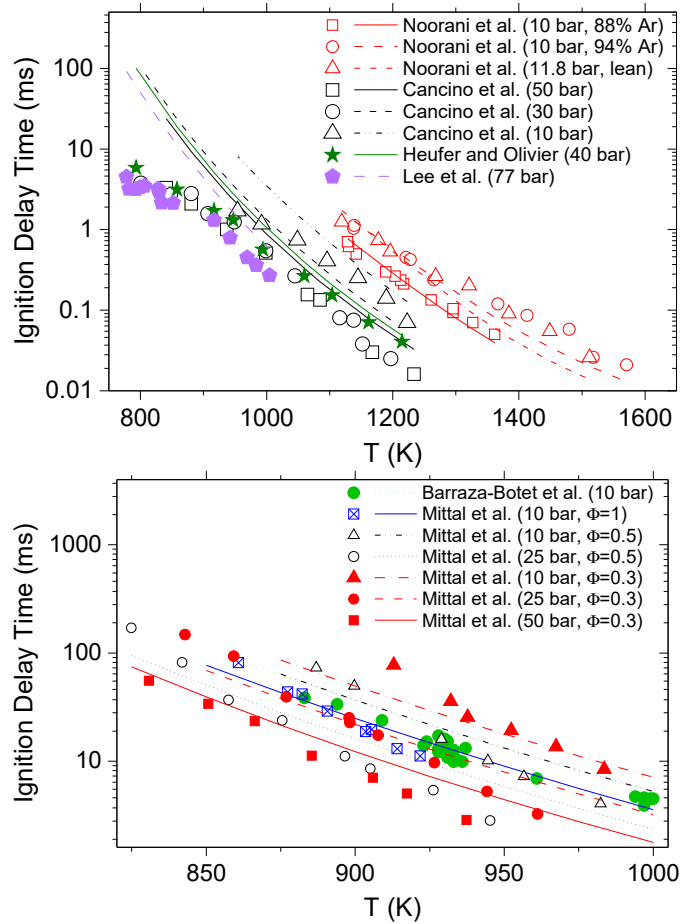
Figure 52: Ignition delay time of stoichiometric ethanol/air from Cancino et al. [84], Lee et al. [86], and Heufer and Olivier [21]; and ethanol/O_2/diluents (Φ=0.3–1) from Noorani et al. [85] (1–2.9% ethanol), Mittal et al. [87] (2.1–6.5% ethanol), and Barraza-Botet et al. [88] (3.6% ethanol). Top fig: measurements from shock tubes. Bottom fig: measurements from RCM. The lines mark the present model prediction.
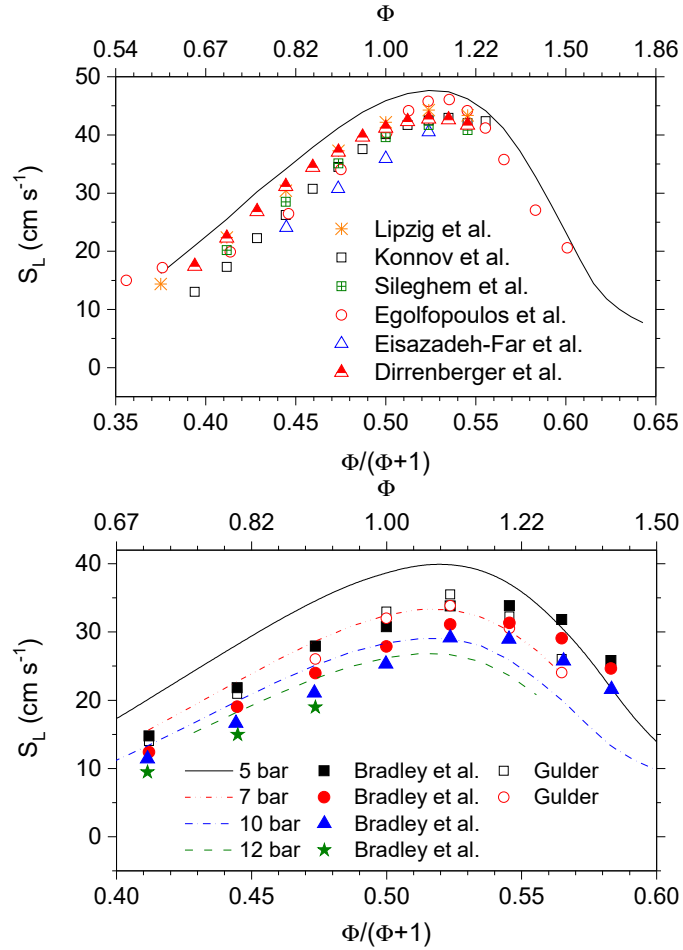
Figure 53: Laminar burning velocity of ethanol/air mixture. Top: atmospheric pressure and initial temperature of 300 K; Bottom: 5–12 bar pressure and initial temperature of 358 K (350 K for data from Gulder [91]). Experimental results are from Gulder [91], Konnov et al. [94], Bradley et al. [93], Lipzig et al. [95], Egolfopoulos et al. [92], Eisazadeh-Far et al. [96], Sileghem et al. [97], and Dirrenberger et al. [98].